Ultrasonic Imaging of the Thyroid Gland

23

Enrico Papini, Claudio Maurizio Pacella,
Andrea Frasoldati, and Laszlo Hegedüs

Diagnostic Ultrasonography

Basic Concepts of B-Mode US

Medical ultrasonography (US) is performed by using a pulse-echo approach. A short, spatially located pulse of ultrasound is produced by a device (*transducer*) and is transmitted into target tissue. US echoes directed back toward the transducer are produced as the pulse travels along a straight path (*ultrasound beam*) through the tissues. As the pulse travels deeper into the tissues, there is a long train of echoes en route back toward the transducer, where they are detected. The different reflectivities of various structures encountered by the pulse cause a corresponding variation of the strength of the echo detection. The detected echo signals are processed and translated into luminance, resulting in a *brightness mode* or B-mode image display. In B-mode images, more reflective structures appear brighter than less reflective ones (*gray-scale resolution*[1]). A complete image is obtained by repeating this pulse-echo cycle for coplanar paths (or *beam lines*). After the echoes from a beam line have been detected by the transducer, further pulses are transmitted for subsequent beam lines. After all the echoes from all the beam lines have been detected and processed, all signals are mapped to the proper locations in the image pixel matrix, and the complete B-mode image is displayed. The entire process is immediately repeated to obtain echoes for the next image frame, generally at rates of 20–40 frames per second (*temporal resolution*[2]).

Basic Ultrasound Physics

Ultrasound consists of mechanical waves with frequency above the upper auditory limit of 20 kHz. Mechanical waves must travel through some physical medium like air, water, or tissue. An ultrasound acoustic wave is a *longitudinal* compressional wave consisting of a series of compressions and rarefactions. The term longitudinal refers to waves that cause oscillatory motion of the medium in the same direction as the direction of wave propagation. The pressure wave moves through the medium at a characteristic propagation velocity for each tissue and depends on the elastic modules and density of the tissue medium. A good average value of velocity of sound in tissue is nominally 1,540 m/s. The sound wave also has a characteristic frequency (number of pressure peaks per second) and wavelength (distance between pressure peaks), both of which depend on the transducer design. Because the velocity is constant, the wavelength (λ) must decrease as the frequency of the sound wave increases. For clinical purposes, it is useful to image with the highest possible frequency because as the wavelength decreases, the axial resolution increases. Medical US devices commonly use longitudinal waves with a frequency range between 2 and 15 MHz.

E. Papini, MD, FACE
Endocrinology Unit, Regina Apostolorum Hospital,
Rome, Albano Laziale, Italy
e-mail: enrico.papini@fastwebnet.it

C.M. Pacella, MD
Department of Diagnostic Imaging and Interventional Radiology,
Regina Apostolorum Hospital, Via S, Francesco, 50,
Rome, Albano Laziale 00041, Italy
e-mail: claudiomauriziopacella@gmail.com;
claudiomaurizio.pacella@fastwebnet.it

A. Frasoldati, MD, PhD
Endocrinology Unit, Arcispedale S. Maria Nuova - IRCCS,
Reggio Emilia, Italy
e-mail: frasoldati.andrea@asmn.re.it

L. Hegedüs, MD, DMSc (✉)
Department of Endocrinology and Metabolism,
Odense University Hospital and University of Southern Denmark,
Kloevervaenget 6, 6th floor, Odense, Funen 5000 C, Denmark
e-mail: laszlo.hegedus@ouh.rsyd.dk

[1] *Gray-scale resolution* is the maximum number of gray shades available in a system, broken into steps from white to black.

[2] *Temporal resolution* is the number of times per second the ultrasound system scans. This is displayed as frames per second.

L. Wartofsky, D. Van Nostrand (eds.), *Thyroid Cancer*, DOI 10.1007/978-1-4939-3314-3_23

Interaction of Ultrasound with Tissue

As ultrasound pulses and echoes travel through tissue, their intensity is reduced (*attenuated*). In general, the amount of *attenuation* increases with the distance from the transducer and with the frequency of ultrasound waves. Thus, imaging of superficial structures (e.g., thyroid or parathyroid glands) demands higher frequencies than deeper lying structures (e.g., liver, kidney, and pancreas). As long as the acoustic characteristics of the tissue in the sound field are constant, the wave will continue to propagate away from the transducer. When tissue with different characteristics is encountered, some of the sound energy will be reflected back to the transducer. The relative amount of energy reflected back depends on the differences between the two tissues. Therefore, echo generation results from the interaction between the incident ultrasound pulse with structures in the tissue medium. Of the different and specific types of interaction, the most important is a tissue property called the *acoustic impedance*. This quantity is correlated with the density of the tissue and velocity of sound in the tissue. Hence, the intensity of the reflected echo increases with increasing impedance difference between tissues. It follows that when the tissues have identical impedance, the result is no echoes. In contrast, all the energy will be reflected when there is a strong difference of acoustic impedance between the tissues (e.g., tissue-air). Interfaces between tissues (excluding the lung and bone) generally produce very-low-intensity echoes. For normal (or 90°) angle of incidence, this type of interaction is called *specular reflection*. If the angle of incidence is not 90°, the echo will not travel directly back toward the transducer but rather will be reflected at an angle equal to the angle of incidence. If the interface between the tissues is rough, the echo will be *diffusely reflected* through a wide range of angles. If the ultrasound pulse encounters reflectors whose dimensions are smaller than the ultrasound wavelength, *scattering* occurs. This results in echoes that are reflected echo intensity through a wide range of angles. On US images most biologic tissue appears as though it is filled with tiny scattering structures. The speckle signal that provides the visible texture in organs like the thyroid gland is the result of interference between multiple scattered echoes. While most of the signal visible in US images results from scatter interactions, the amount and type of reflection depend also on the relationship between the size of the interface and the wavelength. *Reflection* from a large area interface, such as between the liver and the diaphragm (where λ is much less than the object size), is *specular*, like a mirror (the echo travels directly back toward the transducer). Intermediate-size interface (where λ is about the same size as the object) *diffracts* the beam, while small objects, such as blood cells (where λ is much larger than the object size), *scatter* the acoustic wave in all directions. Finally, attenuation is due not only to reflection and scattering but also to friction-like losses resulting from the induced oscillatory tissue motion produced by the pulse, which causes conversion of energy from the original mechanical form to heat. This energy loss is referred to as *absorption* and is the most important component of ultrasound attenuation.

Ultrasound Pulse Formation and Scanning the Ultrasound Beam

A *transducer*, or probe as it is commonly called, is any device that converts energy from one form to another. An ultrasound transducer converts electrical energy to mechanical energy (ultrasound waves). The most important components of ultrasound transducers are piezoelectric elements. The application of electrical waveforms to the piezoelectric elements induces their vibration and the emission of ultrasounds. On the other hand, when sound waves reach the piezoelectric element, they induce vibrations that are converted by the piezoelectric material into electric signals. Thus, an electric current applied across a crystal would result in a vibration that generates sound waves, and, in turn, sound waves striking a crystal would produce an electric voltage. Composite piezoelectric elements commonly consist of tiny rods of lead zirconate titanate ceramic embedded in a matrix of epoxy. Ultrasound pulses that are short in duration and in extent produce US images with the greatest sharpness in the axial direction (axial resolution[3]). Similarly, ultrasound pulses that are narrow in lateral direction produce images with greatest sharpness in that direction (lateral resolution[4]) [1–6].

Most modern US imagers automatically scan the ultrasound beam using transducers consisting of an array of many narrow piezoelectric elements. The array may consist of as many as 128–196 elements [7]. In linear-array transducers, frequently used for US examination of the thyroid gland, the ultrasound beam is created by electrically exciting only a subset of these elements. The ultrasound pulse is emitted perpendicular to the element array and is centered over the element subset. Successive beams are obtained by shifting the subset of excited elements across the face of the array, slightly shifting the beam line laterally. A larger subset of elements is used to receive the returning echoes. The ultrasound beam can be electronically swept across an entire rectangular field in 1/10 s. or faster. The timing is adjusted so that the elements are not all excited simultaneously.

[3] *Axial resolution* defines the ability of the ultrasound transducer to detect two closely spaced reflectors along the direction of sound travel and is directly proportional to the pulse length. The distribution of frequencies present in a beam varies with pulse length: the frequency distribution broadens as the pulse gets shorter. The axial resolution of the imaging system depends on the pulse length: the shorter the pulse length, the better the axial resolution. Short pulses have the broadest frequency distribution but the best axial resolution.

[4] *Lateral resolution* defines the ability of the ultrasound transducer to discern two points perpendicular to the direction of propagation.

Array transducer fields of view (FOVs) are smaller than those produced by past static B-mode scanners, but this disadvantage is compensated for by a more rapid, real-time scanning (*motion mode* or M-mode) that is devoid of motion artifacts.

Echo Detection and Signal Processing

The US image is processed to optimize the appearance on the display. All echo signals are uniformly preamplified after detection by the transducer, and uniform user-controllable *gain* is applied. Equally reflective structures are displayed in the B-mode image with the same brightness, regardless of their depth. The *dynamic range* of the echo signals is also compressed to reduce the gain for larger signal magnitudes and increase the gain for smaller signal magnitudes. These signals are also demodulated to remove oscillations at the ultrasound frequency, and very small signals are removed in order to reduce image noise and clutter. Other steps are designed to obtain sharper edges and improved contrast. Among recent innovations in B-mode US, a mode called *spatial compound imaging* is a new approach to smooth the speckle in order to make the images look less grainy. Spatial compound images smooth the speckle, noise, clutter, and refractive shadows and improve contrast and margin definition [8].

Color and Power Doppler US

The differences in amplitude of backscattered ultrasound produce a gray-scale image, and precise timing allows determination of the depth from which the echo originates. Thus, these differences are related to strength of the interface reflecting the incident sound and are not related to the movement of the target. Rapidly moving targets, such as red blood cells within the bloodstream, produce echoes of such low amplitude that they are not commonly displayed. Nevertheless, the backscattered signal varies from the transmitted signal in frequency as well as amplitude, if the target is moving relative to the transducer. These frequency changes are related to velocity of the moving target by the Doppler equation and are evaluated in the Doppler mode of US signal processing. The Doppler shift is a change in frequency that occurs when sound is emitted from, or bounced off of, a moving object. Movement toward the transducer produces a positive frequency shift, while movement away from the transducer produces a negative frequency shift. The Doppler effect is used to make quantitative measurements of absolute blood velocity and to map blood flow over a large FOV in a semiquantitative manner. Color Doppler (CD) US measurements may be used to determine the presence of flow, determine the direction of flow, identify time-varying velocity characteristics, and detect velocity disturbances. State-of-the-art instrumentation uses intensity and color coding to display complex physiologic and anatomic data to the clinician in a format that can easily be comprehended. The color and intensity represent the direction and magnitude of the velocities present in the image. Analysis of the color flow image gives a graphic illustration of the direction and speed of blood flow within soft tissue. In contrast, power Doppler (PW) considers all frequency shifts to be equivalent, integrating the total amount of motion detected. The assigned color represents the total amount of flow present, independent of the velocity. PW ultrasound is a technique that encodes the power in the Doppler signal in color. This parameter is fundamentally different from the mean frequency shift encoded with CD. The frequency is determined by the velocity of the red blood cells, while the power depends on the amount of blood present. PW has shown several key advantages over CD, including higher sensitivity to flow, better edge definition, and depiction of continuity of flow. The higher sensitivity to slow flow, which is poorly imaged with conventional CD and the improved detailing of the course of tortuous and irregular vessels, has made PW a technique for imaging intratumoral vessels and to improve the accuracy of CD in predicting the likelihood of benign versus malignant nodules. In addition, PD has been used to identify the decreased flow that is characteristic of areas of ischemia, to demonstrate the inflammatory hyperemia, and to assess vascular changes related to therapy [9–14].

Equipment

Accurate ultrasound examination of the superficial structures requires high-frequency broadband transducers, sophisticated electronic focusing, and computing facilities. These instruments provide high-quality B-mode imaging and sensitive Doppler analysis. Broadband technology is useful for systems offering both Doppler analysis and B-mode imaging. The low-frequency component optimizes flow evaluation, while the higher-frequency component allows the study of morphology and structure through gray-scale imaging. High-frequency real-time handheld-specific transducers ranging from at least 7.5 MHz to 15 MHz or more, and focused in the near field, provide enough resolution to discern very subtle differences of acoustic impedance among soft tissues. High-frequency probes can enhance both *spatial resolution* (axial and lateral) and *contrast resolution*[5]. Superficial structures make it possible to increase the frequency of the Doppler signal which is used for both spectrum analysis and color flow mapping (CFM) and to improve the *resolution of vascular structures*[6] [15, 16]. Modern full-size US scanners are relatively portable and inexpensive,

[5] *Contrast resolution* defines the ability to discriminate the differences of acoustic impedance among tissues. It is affected by echo amplitude and tissue attenuation.

[6] *Vascular resolution* describes sensitivity for the detection of very low Doppler signal intensities and Doppler frequency shifts.

especially compared with imaging units for modalities such as MR imaging and CT. Hardware miniaturization and the use of integrated circuitry allow smaller and less expensive US scanners which greatly extends the role of US in the diagnosis and follow-up of thyroid tumors.

How to Perform Thyroid US

The patient is typically scanned in the supine position with the neck slightly hyperextended over a small pillow or a foam wedge. The US machine is usually positioned at the right side of the examining table while the operator is to the right of the patient. For the right-handed operator, the ultrasound equipment is set up such that the right hand does the scanning and the left hand adjusts the scanning features of the machine at the beginning and during the examination. The thyroid gland is initially scanned in both the longitudinal and the transverse planes for a general overview. Next, the entire region is systematically explored in the longitudinal plane starting in the midline to explore the isthmus and then laterally on each side to view the medial, central, and lateral aspects of each lobe as well as the region peripheral to the gland. Each longitudinal scan is performed from the sternal notch to the hyoid region. The common carotid artery and the jugular vein are the useful vascular landmarks that help to define the most lateral or outer border of the thyroid. Still in the longitudinal plane, scanning superiorly beyond the level of the thyroid cartilage depicts cranial structures such as the pyramidal lobe or thyroglossal duct cysts. Next, the entire gland is systematically studied in the transverse plane in the upper, middle, and lower regions of each lobe. Representative images are taken in regions where pathology has been found.

When to Perform Thyroid US

In patients without a palpable nodule, US evaluation of the thyroid gland should be performed when a thyroid disorder is suspected on clinical grounds, when a suspicious cervical adenopathy is revealed by neck palpation, or if risk factors for malignancy (previous head and neck irradiation or a family history of medullary carcinoma, MEN 2A, or papillary thyroid carcinoma in first-degree relatives) are present [17–20]. When a focal lesion of the thyroid gland is revealed by imaging techniques (CT, MRI, PET-CT, or isotope scan), performed for other clinical reasons, a focused US evaluation should be performed to assess the risk of malignancy and the indication for FNA [18–20].

Thyroid US should be performed in all patients with palpable thyroid nodules or goiter to detect US features suggestive of malignancy and to prioritize nodules for FNA. Importantly, US examination additionally provides a reliable measure of the volume of nodules (and the goiter) for follow-up, reveals coexistent thyroid lesions, and aids in the evaluation of differential diagnostic conditions mimicking a thyroid nodule, such as chronic lymphocytic thyroiditis or asymmetrical gland enlargement [21].

A careful US neck examination should always be performed before surgery or radioiodine treatment for a thyroid disorder. US staging provides relevant information about the size of a biopsy-proven malignant nodule, its extracapsular growth, its possible multifocality, and the coexistence of a secondary adenopathy [22, 23].

Thyroid US Reporting

The US report should provide all the information useful for clinical management of thyroid lesions and enable the reader to evaluate the described lesions as for relative risk of malignancy. Qualitative features of thyroid lesions, such as content, type of calcification, border, shape, echotexture, and vascularity – when evaluated in combination – can provide information about the risk of malignancy and should be documented [24, 25]. The following US features of nodules must be reported accurately: (*1*) nodule size, (*2*) internal content, (*3*) nodule shape, (*4*) nodule margins, (*5*) echogenicity, (*6*) calcifications, (*7*) extracapsular invasion, and (*8*) vascularity. While the echotexture of a nodule may be homogeneous or heterogeneous, this feature seems of little help in distinguishing malignant from benign nodules due to low sensitivity and specificity [23, 26].

The nodule *size* should be measured in all three dimensions, but, for minor lesions, usually only the maximal diameter of the nodule can be measured and documented. It is suggested to place the calipers at the outer margin of the halo, when present [27].

The *internal content* of a nodule is generally categorized in terms of the ratio of the cystic portion to the solid component of the nodule: solid (fluid component ≤10 %), predominantly solid (>10 % up to ≤50 %), predominantly cystic (>50 % up to ≥90 %), and cystic (fluid component >90 %) [26]. The nodule may be classified as spongiform when it appears as an aggregation of multiple microcystic components affecting more than 50 % of its volume [26]. The presence of vascularity (Fig. 23.1) or microcalcifications in the solid component should be well documented and stressed in the US imaging report [28–31].

The *shape* of a nodule may be classified as ovoid to round (the anteroposterior diameter of the nodule is equal to or less than its axial diameter on a transverse or longitudinal plane), taller than wide (the anteroposterior diameter of the nodule is longer than its axial diameter on a transverse or longitudinal plane), or irregular, when a nodule is neither ovoid to round nor taller than wide but with a completely uneven shape (Fig. 23.2) [32].

The *margin* of a nodule may be smooth, spiculated (irregular), or ill defined [26, 31–33]. With high-frequency transducer US techniques, previously described ill-defined margins may well be spiculated and jagged edge borders with sharp boundaries (Figs. 23.3 and 23.4).

The *echogenicity* of the solid component of the nodule may be categorized as follows: *marked hypoechoic* when it

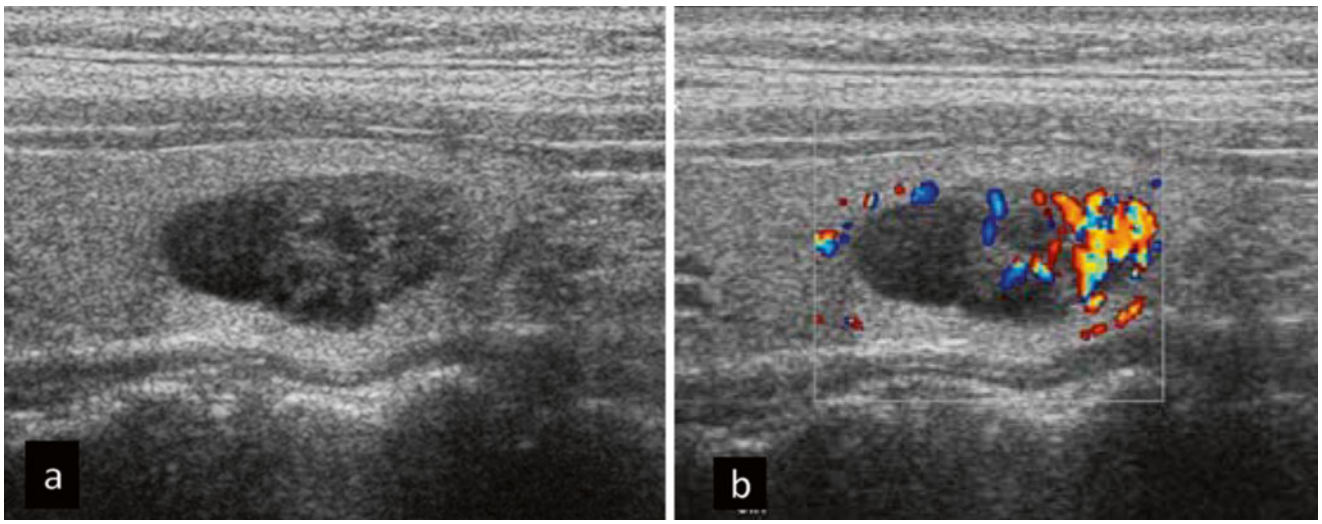

Fig. 23.1 Role of color Doppler US. Sagittal US image of predominantly cystic thyroid nodule with a solid component containing flow. (**a**) Sagittal gray-scale image shows predominantly cystic nodule with solid-appearing mural component. (**b**) Addition of color Doppler mode shows vascularity within the solid mural component, indicating increased likelihood that it is tissue and not debris. US-guided FNA, directed into this zone, showed that it was a papillary carcinoma

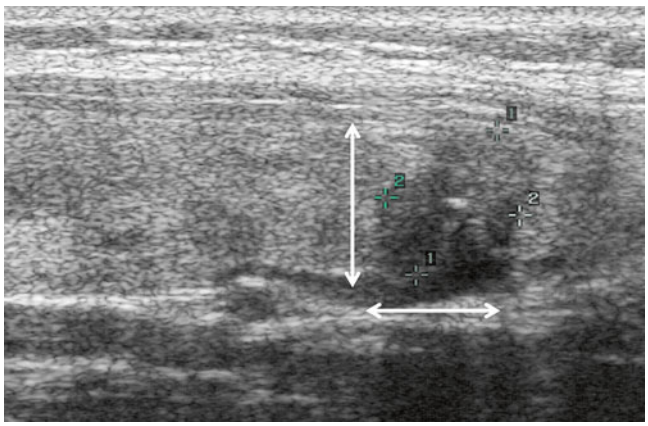

Fig. 23.2 Gray-scale image of a nodule with taller-than-wide shape. US image shows a lesion (*calipers*) with anteroposterior diameter longer than its axial diameter (*arrows*) on sagittal plane. This was a papillary carcinoma

Fig. 23.3 Poorly defined margins of a thyroid nodule. Sagittal US gray-scale image shows blurred and ill-defined margins in the superior part of the nodule (*arrows*). This feature is highly suggestive of malignancy. FNA and surgery confirmed papillary carcinoma. Note also the hypoechogenicity of the lesion

has an echogenicity lower than that of the adjacent strap muscle (Fig. 23.5), *hypoechoic* when the echogenicity of the nodule is comparatively inferior to the surrounding thyroid parenchyma, *isoechoic* when the nodule has the same echogenicity as that of the thyroid parenchyma, and *hyperechoic* when the nodule appears echogenic relative to the surrounding thyroid parenchyma. The latter finding may be present in patients with chronic autoimmune thyroiditis [26].

Calcifications are classified as *microcalcifications* when there are tiny, punctuate echogenic foci of 1 mm or less either with or without posterior shadowing (Fig. 23.6) or as *macrocalcifications* when echogenic foci are larger than 1 mm in size with definite posterior shadowing and as *rim calcifications* when a nodule has peripheral curvilinear or eggshell calcification (Fig. 23.7) [25, 26, 32–37].

As regards the *extracapsular invasion*, the operator should observe carefully at US examination whether nodule margins merge into surrounding thyroid tissue or crosses the thyroid capsule or invades the adjacent structures (usually the perithyroid tissue or, in some cases, the trachea, esophagus, or thyroid cartilage) (Fig. 23.8) [33].

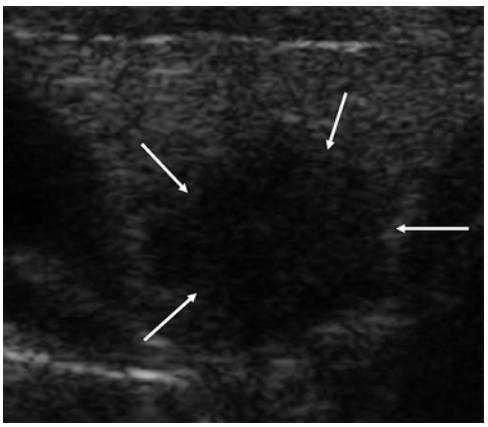

Fig. 23.4 Irregular margins in a thyroid nodule. Sagittal US gray-scale image shows spiculated and jagged margins (*arrows*) of the nodule. In addition, the nodule appears markedly hypoechoic. FNA and surgery confirmed that it was a papillary carcinoma

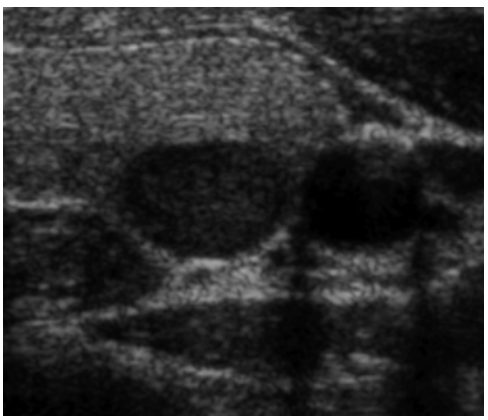

Fig. 23.5 Marked hypoechogenicity of a thyroid nodule. Transverse gray-scale US image shows a nodule with regular margins but marked hypoechogenicity. This was a papillary carcinoma both at cytology examination and at surgery

CD US and PW US are well suited for the evaluation of the intralesional *vascularity* of thyroid nodules (Fig. 23.9) [38, 39].

If US evaluation reveals the presence of multiple nodules, a short general description of the thyroid size and structure and of the number and size of the nodules is suggested. However, the report should be specifically focused on the nodule(s) with US features associated with risk of malignancy and on the presence/absence of suspicious lymph nodes or signs suggestive of extracapsular growth [23].

US Criteria of Malignancy

US Features Suggestive of Malignancy

The risk of malignancy, at the individual level, is independent of whether the patient has a single or multiple palpable thyroid nodules [33], but the challenge of diagnosing it in the latter may be pronounced [17, 40]. One of the major reasons for the increasing use of diagnostic imaging, and imaging-guided FNA, is the wish to offer nonsurgical therapeutical alternatives to the vast majority of patients (>95 %) who are in need of therapy but do not have thyroid malignancy [17–19]. Unfortunately, there is a significant overlap of the US features between benign and malignant thyroid lesions. On the basis of several retrospective and prospective reports [27, 32, 33, 35, 36, 41–43] and two recent South Korean studies [26, 44], the *features predictive of malignancy* in thyroid nodules can be categorized as follows [17]:

- Taller-than-wide shape (sensitivity 40–64 % and specificity 91–100 %).
- The presence of margin abnormalities (microlobulated or spiculated margins) (sensitivity 48–69 % and specificity 92–98 %).
- Marked hypoechogenicity (sensitivity 41–64 % and specificity 92–98 %).
- The presence of microcalcifications (sensitivity 40–44 % and specificity 91–98 %).
- Evidence of aggressive growth (extension of the lesion beyond the thyroid capsule, invasion of the strap muscles, or infiltration of the tracheal cartilage). This is infrequent, but with nearly 100 % specificity for malignancy.
- Coexistence of suspicious lymphadenopathy (enlarged neck lymph nodes with no hilum, cystic changes, and/or microcalcifications) (sensitivity 18 % and specificity 100 %). Lymph nodes with a rounded hypoechoic appearance and hypervascularity are a more frequent but less specific finding [45].

US findings *suggestive of a benign thyroid lesion*:

- Spongiform appearance (sensitivity 10 % and specificity 100 %)
- Isoechoic US appearance (sensitivity 57 % and specificity 88 %)
- Well-defined smooth and regular margins (sensitivity 61 % and specificity 74 %)
- Purely cystic lesion (specificity 100 %).

Borderline features that are associated with thyroid carcinoma but with a low diagnostic accuracy are:

- Hypoechogenicity (sensitivity 11 % and specificity 78 %)
- Macrocalcifications (intranodular macrocalcifications and interrupted eggshell calcifications) (sensitivity 10 % and specificity 86 %)
- Predominant central vascularization (sensitivity 6 % and specificity 89 %)

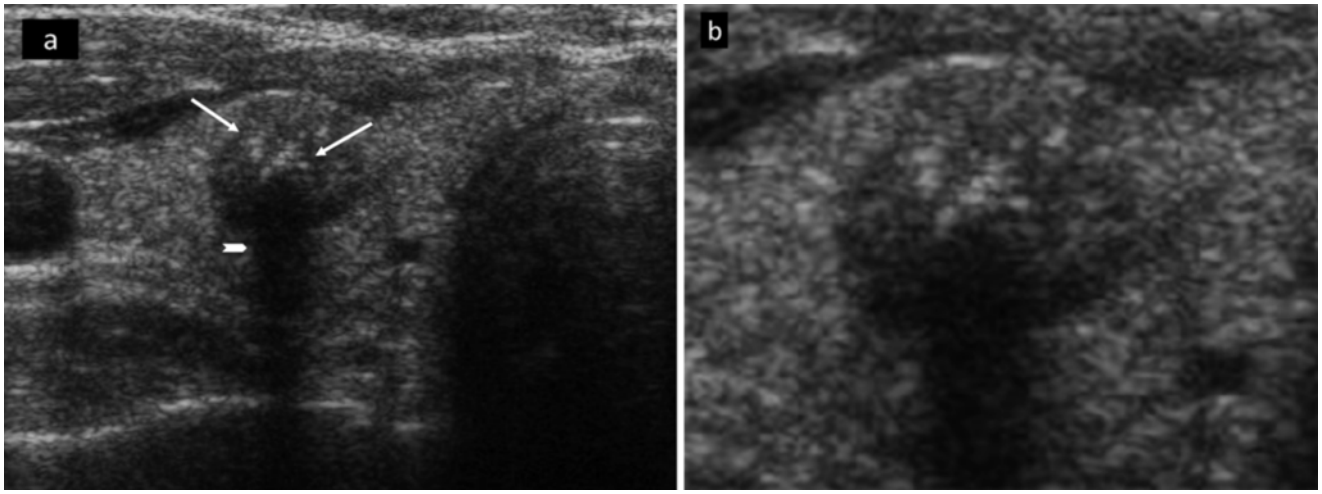

Fig. 23.6 Postsurgical neuroma in a patient previously treated by thyroidectomy and lateral neck dissection. The lesion is superficially located and appears as an oval, slightly inhomogeneous lump, with a hyperechoic posterior margin (Panel **a**). At one pole, the hypoechoic and almost avascular structure continues in an elongated tail (Panel **b**)

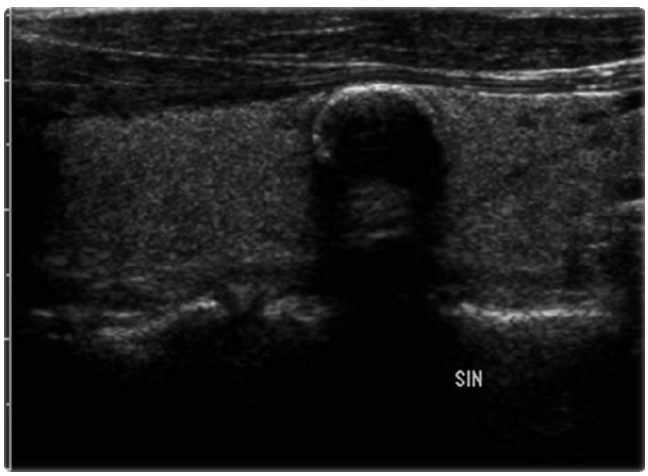

Fig. 23.7 Peripheral curvilinear or eggshell calcification in a thyroid nodule. Sagittal gray-scale US image shows peripheral partial curvilinear calcification in the superior part of the lesion with evident posterior shadow. This US finding is suggestive of a benign thyroid lesion

A taller-than-wide shape is highly predictive of malignancy because it is the expression of a centrifugal growth of the nodule across the tissue plane, while benign lesions usually enlarge along a direction that is parallel to the tissue plane. Unfortunately, an ovoid to round shape is only partially suggestive of a benign nodule because papillary microcarcinomas may appear as well-defined round hypoechoic lesions.

The finding of irregular margins is strongly predictive of malignancy, because it is the expression of an infiltrative growth. Ill-defined or poorly defined margins may be seen in both benign and malignant nodules. Benign thyroid nodules, indeed, are known to be incompletely encapsulated and poorly marginated, and they can merge with normal tissue [46].

Hypoechogenicity is a marker of risk of malignancy, since most thyroid carcinomas are characterized by a hypoechoic US appearance. However, many benign nodules are hypoechoic as well, and only marked hypoechogenicity is strongly predictive of malignancy.

The presence of intranodular microcalcifications, due to psammoma bodies (laminar calcific deposits within the tumor papillae), is highly predictive of papillary thyroid carcinoma. Unfortunately, the high specificity of this finding is associated with a rather low sensitivity [46]. Macrocalcifications are frequently encountered in medullary thyroid carcinomas and in anaplastic carcinomas, but they are more often seen as a consequence of tissue necrosis in benign long-standing nodular goiters.

The vascularity pattern, using CD or PW US, is of little help in differentiating benign from malignant nodules [47, 48]. Intratumoral hypervascularity is frequently detected in thyroid carcinomas, but the presence of intranodular vascular signals is a highly nonspecific finding. Perinodular flow is mainly a characteristic of benign nodules, but it is detected in a nonnegligible number of malignant nodules as well. Probably only a few qualitative features, like the presence of a marked chaotic intranodular vascularization or of large penetrating "swordlike" vessels, may be of use in selected malignant lesions [49].

The size of the nodule and the rate of growth in most cases do not distinguish a benign from a malignant nodule [21, 33]. Many benign nodules are characterized by a slow but progressive volume increase during long-term follow-up, and only aggressive tumors (poorly differentiated and anaplastic carcinomas, thyroid lymphomas, and sarcomas) demonstrate a rapid growth over a period of weeks or months [50].

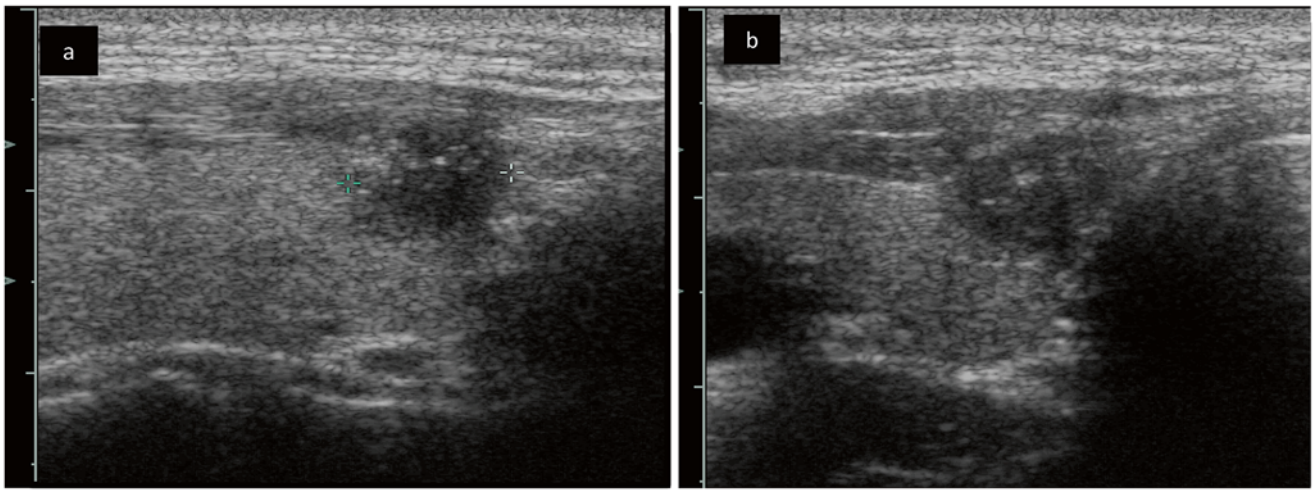

Fig. 23.8 Representative cases of nodules with evidence of aggressive growth. (**a**) Transverse US B-mode image shows a hypoechoic nodule (*calipers*) with irregular margins and intralesional microcalcifications that cross the thyroid capsule and invade the adjacent perithyroid structures. (**b**) Transverse US image shows a nodule with intralesional microcalcifications that invade perithyroid tissue and the contiguous tracheal wall. Cytology and surgery confirmed papillary carcinoma in both cases

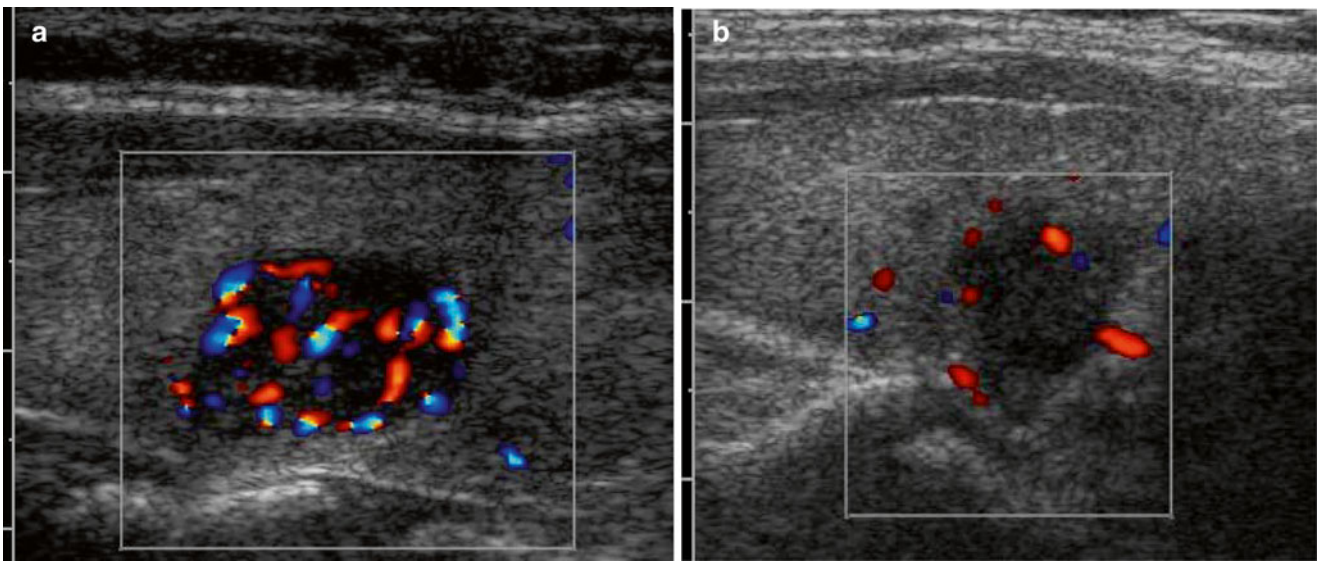

Fig. 23.9 Role of color Doppler US. (**a**) Color Doppler mode shows marked internal vascularity, indicating increased likelihood that the nodule is malignant. (**b**) Color Doppler mode shows little internal vascularity in a markedly hypoechoic nodule with irregular margins. Cytology and surgery confirmed papillary carcinoma, in both cases

Pure cysts are invariably benign, but partially cystic thyroid lesions are reported as malignant in 5–26 % of cases [30]. US evidence of a relevant solid component with marked vascular signals or microcalcifications should raise suspicion of a partially cystic carcinoma.

When to Perform US-Guided Thyroid Biopsy

FNA biopsy should be performed:

- In patients with a history of neck irradiation or family history of papillary thyroid carcinoma, medullary thyroid carcinoma, or multiple endocrine neoplasia type II. This should be performed independent of nodule size, if technically feasible.
- In patients with US findings suggestive of extracapsular growth or with metastatic cervical lymph nodes. This should be performed independent of nodule size, if technically feasible.
- In patients without a high-risk history and with nodules smaller than 10 mm, only in the presence of at least one suspicious US finding.
- In patients without a high-risk history and with nodules greater than 10 mm but smaller than 20 mm, only in the presence of at least one borderline US finding.

- In all patients with nodules greater than 20 mm or with progressive growth.
- In patients with thyroid incidentalomas detected by PET-CT with ^{18}F-fluorodeoxyglucose or with Tc99m sestamibi scan.

Interventional Ultrasonography

US-Assisted Thyroid Biopsy

FNA is the pivotal procedure for the assessment of malignancy risk of thyroid nodules and cervical lymph nodes. US guidance of FNA is necessary for cytological sampling of nonpalpable nodules and of lesions in anatomically difficult sites. Routine use of US-guided FNA is strongly recommended in palpable thyroid nodules as well, due to the increased diagnostic accuracy and the decreased risk of complications [19]. A team comprising an operator and a trained nurse can reliably perform US-guided FNA. The US machine should be equipped with a linear transducer with a 3.5–4.0 cm footprint and multiple frequency settings ranging between 7.5 and 14 MHz and CD/PW capability. Small curvilinear transducers may be useful for imaging otherwise inaccessible locations, especially in the lower neck The clinical usefulness of an elastosonography software is still under evaluation and debated [51, 52].

The operator is situated on the left side of the patient, and the assistant, or the nurse, stands on the right side. The US equipment is placed on the right side of the patient at the level of her head. The assistant is required to handle the US machine switches, such as freeze, depth, gain, color, and power color adjustments. The operator holds the transducer with the left hand and watches images on the monitor in front of her, aims the guide to the target, and inserts the needle with the right hand. If the procedure is carried out by two physicians, the operator can perform the biopsy maneuver while the assistant holds the transducer and supervises the needle track. The monitor should be placed in front of the operator, allowing a straight comfortable field of vision. A setup tray should include the material for topical cleansing, transducer sterile covers, sterile coupling gel, syringes (from 5 to 20 ml), and hypodermic needles of different gauges (G) and lengths. FNA is usually performed with 25–27G needles, but the sampling of dense, fibrotic lesions is better accomplished with 22–23G needles. The drainage of sticky colloid collections may require even larger needles up to 19–20G. Spinal or stylet-type needles are more expensive than ordinary needles, but in selected cases, they are of use since they avoid the uploading into the needle lumen of gel, blood, or follicular cells from normal thyroid parenchyma while advancing the needle toward the lesion of interest. Needles of variable length are required. Spinal needles inserted through the needle guide should be 75–90 mm long, while shorter needles are used for US-assisted procedures in cases where a guide attachment is not required.

Pistol grip holders allow the operator to use the left hand to hold the transducer for direct control of the target view and the right hand to fit and move the needle. This procedure allows continuous real-time vision of the target. A detachable needle guide, adapted for the transducer, may permit the operator to act on his own, with the assistance of a nurse. When using syringe holders, the operator should carefully avoid to apply an excessive aspiration pressure, especially on highly vascularized thyroid lesions. In these cases, the optimal sampling is obtained without any or with very little suction.

A worktable prepared with glass slides and fixing materials (95 % alcohol solution bottles for slide glass immersion or isofix spray) should be available for immediate smearing and fixation. If the physician has no or limited experience in the sampling maneuver and slide smearing, the entire procedure is at risk of failure. The expression of the sampled material into transport media, for subsequent liquid-based cytology or cell block preparation, is preferable in such situations.

Waste boxes to dispose needles and biologic material should be at hand. Two 4 ml tubes, containing normal saline solution 1 ml, should be available for the analysis of relevant biochemical markers in the needle washout (thyroglobulin, calcitonin, parathyroid hormone, and other markers).

An extended field of view of the thyroid gland should be obtained before the biopsy procedure. A careful preliminary US evaluation allows the operator to choose the most relevant lesion(s), the best percutaneous approach, and the length and type of needle. A Doppler imaging assessment of the gland rules out the presence of large intrathyroid vessels along the supposed path of the needle and provides information about the lesion's vascularity.

The transducer is enclosed in a plastic cover or Parafilm to avoid contact of the probe with the patient's blood. The skin of the neck is cleaned with antiseptic solution. Local anesthesia with subcutaneous injection of 2 % lidocaine, or with an anesthetic spray, is usually unnecessary for FNA performed with 25–22G needles. When warranted, lidocaine should be injected from the subcutaneous tissue down to the strap muscles and the thyroid capsule.

The US-guided FNA procedure can, basically, be performed with a "parallel" or a "perpendicular" approach [53]. According to the parallel approach, the needle is inserted at either of the short sides of the probe, and it is angled down toward the nodule. The parallel approach has the advantage to show nearly completely the track of the needle from its insertion into the skin until its penetration into the target lesion. This approach is best suited for procedures performed

with a guiding device because the path of the needle must be continuously maintained in the scan plane of the transducer while the tip advances toward the lesion.

The perpendicular approach requires two experienced operators because the tip of the needle is visualized only in the final phase of the procedure. Both the point of needle insertion into the skin and the nodule to be aspirated must be carefully centered at the midpoint of the long axis of the probe. The needle must be inserted with the precise angle of descent (usually a 30–40° angle with the vertically placed transducer) to allow placing the needle tip into the nodule. As the initial part of the needle course is not visualized, the operator should be able to predict the needle path in order to avoid an excessively cranial or caudal placement of the needle bevel [54].

US-guided FNA may obtain material from a nodule by means of "aspiration" (or closed suction) or by "nonaspiration" (or needle-only) techniques [55, 56]. According to the aspiration technique, a 22–25G needle attached to a 10–20 ml syringe is inserted into the lesion and only after the correct placement of its tip is a gentle aspiration performed, withdrawing the plunger of the syringe for a 1–5 ml volume. The needle is rapidly moved back and forth within the lesion for 5–10 s, then the syringe plunger is completely released, and the needle is quickly withdrawn from the neck. The needle is disconnected, 5 ml of air is aspirated into the syringe, the needle is reinserted, and the aspirated material is expressed onto a glass slide for smear or into a transport medium for liquid-based cytology. This technique is rapid and effective for most solid thyroid nodules and especially for the nonpalpable or deeply located lesions.

The nonaspiration technique is of use for highly vascularized nodules and for complex lesions with a component of degeneration and/or fluid. The hub of a 25–27G needle is held by the operator with her fingertips in a pencillike way and is inserted within the lesion while performing rapid back and forth movements according to the aforementioned procedure. After about 5 s, a fingertip is placed over the needle hub to close it, the needle is withdrawn, and it is attached to a syringe with an already retracted plunge. This procedure leads to a capillary-driven uploading of material into the needle. The absence of any aspiration avoids the dilution of the cellular material with colloid fluid or blood. In deeply located lesions, the procedure can be performed with a spinal needle that is attached to a 10–20 ml syringe with its plunge partially retracted or removed.

The recommended biopsy sites are as follows [40]:

- In large nodules, the peripheral part of the lesion rather than the central area, in order to escape sampling degenerative changes and fluid collections which may hamper sample adequacy.
- In entirely cystic areas, the center of the lesion should be reached in order to drain the fluid content completely. Cyst fluid should be submitted to the laboratory within the syringe for evaluation after centrifugation. Most colloid fluids are clear yellow with minimal blood staining. Clear-colorless fluid suggests the sampling from a parathyroid gland and parathyroid hormone should be measured. Bloody liquid is usually drained from hemorrhagic pseudocysts, and this finding may represent a malignant lesion, although most often it is not.
- In mixed thyroid nodules, before the drainage of the fluid component, a careful sampling should be performed from the solid pedicles growing into the cystic lumen. The needle tip should be aimed at hubs that are vascularized at PW examination or at their basis, because the extremities of the pedicles usually contain mostly necrotic debris and degenerative changes. After a complete drainage of the fluid, both the solid areas and the peripheral borders of the lesion should be sampled.

Ideally, the request form for the cytopathology laboratory should provide the following clinical data: location and size of the nodule, suspicious US findings, thyroid function including the presence of autoimmunity and calcitonin level – if available, current medical treatment, history of neck irradiation, and personal or family history of thyroid malignancy. Suspicion of malignancy, whether clinical or based on the US findings, should always be expressed.

US-Guided Core Biopsy

The role of FNA in the initial evaluation of thyroid nodules is widely accepted. However, inadequate or suboptimal specimens constitute major limitations. Inadequate specimens are obtained in up to 15–25 % of FNA procedures, and suboptimal samples, due to insufficient cellularity or blood contamination, are even more frequent. Core needle biopsy (CNB) is an US-guided biopsy aimed at obtaining a small size tissue sample for histological evaluation by means of a 22–20G cutting needle. The procedure is usually performed with disposable spring-activated devices widely available on the market. These needles are small enough to precisely sample thyroid lesions in the 8–20 mm range with a very low risk of local bleeding or of damage to the cervical structures [40].

CNB should be performed under US guidance and by experienced operators only. After skin cleansing with an antiseptic solution, a careful local anesthesia with the injection of 2 % lidocaine from the subcutaneous tissue down to the muscle layers of the neck and the thyroid capsule is required to reduce local pain.

For a safe procedure, the longitudinal (craniocaudal) approach is recommended, because this needle track is not directed toward vital structures of the neck (large vessels or

trachea). The needle is inserted into the lesion under US monitoring, and the absence of local bleeding should be ensured during the insertion through US images in different planes. The needle tip should never break outside the lesion before needle firing. After careful placing of the needle and instructing the patient not to swallow or speak, the needle is triggered and rapidly extracted [57, 58].

Material may be traditionally processed by fixation of the tissue in formalin for hematoxylin and eosin examination and/or gently crushed between two slides to prepare an air-dried sample for cytological examination [59]. Pressure and ice pack should immediately be placed on the biopsy site to prevent local bleeding, pain, and discomfort. An oral analgesic effectively controls pain, if present. An US control after 30 min, mainly to rule out hemorrhage, is suggested before patient discharge.

The rate of unsatisfactory thyroid nodule sampling with CNB has been reported as low as 3.4 % and importantly without significant procedure complications [59]. Thin-needle CNB provided an impressive 98.3 % adequacy rate in a series of 258 patients with a previous unsatisfactory FNA sampling [60].

CNB is a safe technique, when performed by experienced operators, and may be recommended in solid thyroid nodules which despite repeated (usually two) FNAs has yielded unsatisfactory samples. CNB may be performed simultaneously with FNA when one or two aspiration samplings have yielded insufficient or suboptimal material from fibrous nodules or lesions with a rubbery consistence (such as chronic lymphocytic thyroiditis). CNB may be the first-choice procedure in case of unusual thyroid lesions that are suspicious for metastatic tumors, lymphoma, sarcoma, or undifferentiated thyroid carcinoma. In all these cases, CNB may provide some architectural definition as well as a quantity of material enabling immunohistochemical or molecular biology evaluations.

US-Assisted Mini-invasive Procedures for Thyroid Malignancy and Neck Recurrence

Most differentiated thyroid carcinomas are cured by the initial surgical treatment, which is usually followed by radioiodine ablation. However, some patients with thyroid carcinoma are found to have neck lymph node metastases during their long-term clinical and US follow-up. The recurrence rate within a 30-year follow-up is reported to be as high as 9–20 % in patients with differentiated thyroid carcinoma and up to 25 % in patients with medullary thyroid carcinoma. In some of these cases, radioiodine treatment is not effective in eradicating nodal metastases due to their scanty or absent 131-I uptake. In such situations, current US techniques make it possible to identify subcentimetric and clinically occult cervical metastases, which can rapidly be confirmed by US-guided FNA but which may be beyond surgical reach. Additionally, a few of these patients have previously undergone repeated neck explorations, and when further metastases are revealed, their resection is cumbersome and confer a high risk of surgical complications due to the extensive neck scarring. Based on these considerations, and on the commonly indolent course of neck metastases from thyroid carcinomas, the use of nonsurgical ablation techniques has been proposed and is currently under evaluation for the treatment of cases at high surgical risk of complications [61].

Percutaneous Ethanol Injection

Percutaneous ethanol injection (PEI) was first used for the chemical ablation of small hepatocellular carcinomas [62]. Ethanol induces coagulation necrosis of the lesion as a result of cellular dehydration, protein denaturation, and chemical occlusion of small lesion vessels. PEI has also been proposed as a nonsurgical treatment of secondary/tertiary hyperparathyroidism [63] to ablate parathyroid tissue [64, 65]. Subsequently, PEI has been employed to treat both hyperfunctioning nodules and benign cold nodules of the thyroid gland [66, 67]. Due to technical limitations, short- and long-term complications – mainly caused by ethanol seepage along the needle tract – as well as recurrences due to incomplete ablation, the therapy has been abandoned by all the centers that initiated the therapy in the first place [68]. At present, the only remaining indication for PEI is treatment of cysts or predominantly cystic lesions [21, 69–71].

In 1999, PEI was first proposed as a palliative treatment in a case of inoperable thyroid carcinoma [72]. Subsequently, PEI has been evaluated as a possible treatment for thyroid cancer metastases in cervical lymph nodes in patients who were not candidates for surgical resection or radioiodine therapy [73]. In a series of 14 patients with 29 neck nodal metastases (NNM) from papillary thyroid cancer (PTC), US follow-up after PEI showed a mean volume decrease from 492 mm^3 at baseline, to 76 mm^3 after 12 months, to 20 mm^3 after 24 months [73, 74]. In a second series of 20 patients with 23 nodal metastases, six lesions disappeared completely after PEI, while seven lymph nodes required a second treatment. A complete control was reported in 15 patients with an average injection of only 0.7 ml of ethanol [75]. In a third trial, six patients with biopsy-proven neck recurrences of well-differentiated thyroid cancer were treated with PEI and had 18.7 months' clinical and US follow-up. Four patients showed a rapid reduction of the volume of their metastatic lymph nodes, while two of them needed repeated treatments. No neck disease persistence was reported, and serum thyroglobulin levels dropped from a mean pretreatment value of 6.1–2.0 ng/ml [76].

Lim et al. [77] used US-guided PEI on 24 recurrent lesions (eight in thyroid beds and 16 in neck nodes) of 16

papillary thyroid carcinoma patients. Ethanol was injected at 3-month intervals under US guidance. The median diameter of the lesions was significantly reduced, from 9.9 mm (range 5.5–25.0 mm) to 5.3 mm (range 0.0–17.0 mm) by PEI. Four recurrent lesions disappeared sonographically. Kim et al. [78] treated 27 patients with 47 cervical metastases by PEI with a mean follow-up of 28.2 (14–38 months). Ethanol (99 %) was repeatedly injected with adjusting needle position until the entire lymph node was ablated. All metastases significantly decreased in volume (range 30–100 %; mean 93.6 %). The mean number of sessions, the total volume of ethanol per NNM-PTC, and the mean volume of ethanol per session per NNM-PTC were 2.1 sessions (range 1–6), 2.4 ml (range 0.3–10.1), and 1.1 ml/session (range 0.3–3.0), respectively. More recently, Heilo et al. [79] described their experience in 69 patients with 109 neck metastases of papillary thyroid carcinoma. A total of 101 of the 109 (93 %) metastatic lymph nodes responded to PEI treatment, 92 (84 %) completely, and 9 incompletely. Two did not respond, and four progressed. Two lymph nodes previously considered successfully treated showed evidence of malignancy during follow-up. Serum TG values were available from 62 patients before PEI and from 60 at the end of follow-up. Of 51 patients without TG antibodies, 13 had undetectable serum TG levels (<0.2 μg/l) before PEI, despite biopsy-proven metastatic disease. Of the 38 patients with elevated serum TG values before PEI, 30 patients had undetectable values after PEI treatment.

Although the procedure has proven to be quite safe, and few complications have been reported [76–79], PEI treatment of neck lesions devoid of a capsule is usually characterized by a transient but sharp pain radiating to the jaw and the chest, likely related to the leakage of ethanol into surrounding cervical soft tissue. Potential complications to PEI include damage to the recurrent laryngeal nerves or the parathyroid glands. In addition, a posttreatment local fibrosis is frequent. A relevant limitation of PEI, for ablation of cancer recurrences, is the difficulty of achieving – with a single treatment – a definite area of coagulative necrosis with certainty associated with complete ablation of the target tissue. Ethanol diffusion is unpredictable, and there is no precise correlation between the amount of ethanol injected into the lesion and the size of the coagulative zone [69]. While the aforementioned data look convincing, it is important to recognize that there is ongoing discussion of whether PEI should be employed for this purpose. Most centers do not and there are no data on cost-effectiveness and whether the procedure influences quality of life or the prognosis of the patients.

Radiofrequency Ablation

The goal of radiofrequency (RF) ablation is to induce thermal injury to the tissue through electromagnetic energy deposition. In the more popular monopolar mode, the patient is part of a closed-loop circuit that includes a radiofrequency generator, an electrode needle, and a large dispersive electrode (ground pads). An alternating electric field is created within the tissue of the patient. Because of the relatively high electrical resistance of tissue in comparison with the metal electrodes, there is marked agitation of the ions present in the target tissue that surrounds the electrode. This is due to the tissue ions attempting to follow the changes in direction of alternating electric current. The agitation results in frictional heat around the electrode. The discrepancy between the small surface area of the needle electrode and the large area of the ground pads causes the generated heat to be focused and concentrated around the needle electrode. Several electrode types are available for clinical RF ablation, including internally cooled electrodes and multiple-tined expandable electrodes with or without perfusion [80, 81].

RF was first applied to a group of eight patients with locally recurrent well-differentiated thyroid carcinoma (WTC) [82]. The mean diameter of the lesions was 2.4 cm, and the treatment was performed under US guidance and using intravenous conscious sedation. The RF electrode was inserted into the site of the recurrent lesion and treated with the maximum allowable current for between 2 and 12 min. All patients were treated as outpatients. A minor skin burn and one case of vocal cord paralysis occurred. With a mean follow-up of 10 months, no recurrent disease at the treatment site was detected [82]. Subsequent histological examination showed no evidence of a tumor in the treated lymph nodes in six patients [82]. The same center reported a second series (not specified if in part coincident) [76] of 12 patients who underwent RF treatment of biopsy-proven recurrent thyroid carcinoma in the neck. No recurrent disease was detected at the treatment site in over 80 % of the patients after a mean follow-up of 41 months. A minor skin burn and one permanent vocal cord paralysis occurred after RF treatment. Thus, RF ablation shows promise as an alternative to surgical treatment of recurrent differentiated thyroid carcinoma in patients at surgical risk. Clearly, adequately controlled long-term studies are necessary to determine the possible role of RF in the treatment of recurrent malignant thyroid tumors.

Laser Ablation

The term “laser ablation” should be used for ablation with laser light energy applied via fibers directly inserted into the tissue. A great variety in laser sources and wavelengths are available. In addition, different types of laser fibers, modified tips, and applicators can be used. A spherical volume of coagulative necrosis up to 2 cm in diameter can be produced from a single, bare 300–400 μm laser fiber. Two methods have been developed for producing larger volumes of necrosis. One utilizes firing multiple bare fibers arrayed at 1.5–1.8 cm spacing throughout a target lesion [80, 81, 83–86]. The other employs cooled-tip diffuser fibers that can deposit

up to 30 W over a large surface area, thus diminishing local overheating [80, 87–89].

Laser ablation (LA) has been tested in undifferentiated thyroid carcinomas. The first reported case was a 75-year-old woman with a rapidly progressive anaplastic thyroid carcinoma [90]. After achieving the ablation of a large proportion of the tumor, an external beam radiation therapy was performed. The volume of the tumor and local symptoms (dysphagia and cervical pain) were markedly reduced and stabilized during the following 4 months. A similar, albeit transient, improvement was reported in another inoperable anaplastic carcinoma patient with an aggressive course [91].

Recently, with a 1,064 nm Nd:YAG laser source operating in continuous wave mode, using 300 μm plane-cut optic fibers inserted through the sheath of two 21 gauge spinal needles and a total energy of 3,600 J, an incidental solitary papillary microcarcinoma (PTMC) of 8 mm in maximum diameter, confined to the thyroid gland, was completely ablated in an elderly patient at high surgical risk. US-guided FNA and a core-needle biopsy performed at 1 and 12 months after the procedure showed necrotic material and absence of viable neoplastic tissue. A contrast-enhanced US (CEUS) scan performed after 24 months showed that the neoplastic lesion was completely replaced by a large avascular hypoechoic area [92].

Solbiati et al. [93] used the same technique [83, 94] to treat 23 metastatic nodes (mean size 1.2 cm; range 0.6–2.6 cm) from papillary cancer of the thyroid gland in 19 patients who had previously (13–54 months earlier) undergone thyroidectomy and central and laterocervical lymph node dissection. All cases were negative at ^{131}I whole-body scan but had marked uptake at 18F-FDG PET and elevated serum levels of TG. Lymph nodes were treated with one or two [6] fiber insertions, each one with a power of 3 W for 400–600 s (total energy applied 1,200–1,800 J). After withdrawing the fiber, CEUS was performed to assess the lack of enhancement in the treated lesion. All cases were followed at 3 and 6 months with B-mode US, CEUS, 18F-FDG PET, and assessment of serum levels of TG. In 21 of 23 (91.3 %) cases, complete ablation (disruption of the parenchymal structure at B-mode US, lack of enhancement at CEUS, no uptake at 18F-FDG PET with normalization of peak standard uptake value (SUV) (Fig. 23.10), and >90 % decrease of TG serum levels) was achieved. In two cases, residual uptake at 18F-FDG PET with abnormal SUV was found, and laser ablation was repeated and subsequent normalization of all parameters was achieved.

LA treatment of four cases of local recurrence of poorly differentiated thyroid carcinoma has been described [95, 96]. All patients were elderly and had previously had total thyroidectomy followed by cervical lymphadenectomy and external beam radiation therapy for repeated cervical recurrences. Neck metastases were not iodine avid and symptoms of local invasion (cervical pain, dysphagia, and dysphonia) were present and progressive. In all cases, from two to five LA treatments were performed during a mean period of 20 months, which induced a marked tumor shrinkage and a clinically significant improvement of local symptoms. LA was combined with a further cycle of external beam irradiation in two patients and with a bronchoscopic laser treatment for control of tracheal invasion in one case. Laser procedures were well tolerated and only caused mild cervical pain, which was controlled by betamethasone and ketoprofen given for 24 h. No major complications were recorded [95, 96].

Despite the limited number of cases, percutaneous US-guided LA is a promising therapeutic tool for PTMC ablation in fragile patients at high surgical risk and for neck metastases from differentiated thyroid carcinoma in patients already treated with repeated lymphadenectomy. Thermal ablation may be used for local recurrences of poorly differentiated or medullary thyroid carcinomas that are not amenable to traditional surgical treatment, for improving local compressive symptoms, and for inducing a decrease of the volume of neoplastic tissue prior to external radiation therapy or target therapy [61].

Although not the focus of this chapter, we have to stress the important outcomes achieved by these hyperthermic techniques when treating, percutaneously, benign thyroid lesions. US-guided thermal techniques result in a satisfactory long-term clinical response with improvement in pressure symptoms and cosmetic complaints in the majority of the patients with a benign solitary solid thyroid nodule [97–102].

High-intensity focused ultrasound (HIFU), a technique which delivers US-guided thermal destruction without penetration of the skin, has recently shown promise in the therapy of small benign nodules in the thyroid [103, 104]. In principle, this technique holds promise also for ablating malignant thyroid tissue.

Perspectives

Ultrasound Elastography of the Thyroid

Principles

Thyroid nodules that are hard and fixed at physical examination are well recognized as clinically suspicious [40]. The B-mode US examination of the thyroid offers a valuable guide for assessing the risk of malignancy of thyroid lesions, but it does not provide any information about its hardness. Hence, the hardness of nonpalpable thyroid nodules cannot be evaluated by either US or palpation. US elastography (sonoelastography) is a noninvasive imaging technique that can be used to map relative tissue stiffness or displacement (strain) in response to an imparted force [105, 106]. Stiff tissue deforms less and exhibits less strain than does compliant tissue, in response to the same applied force. Thus, the basis of elastography is analogous to manual palpation [106]. This novel

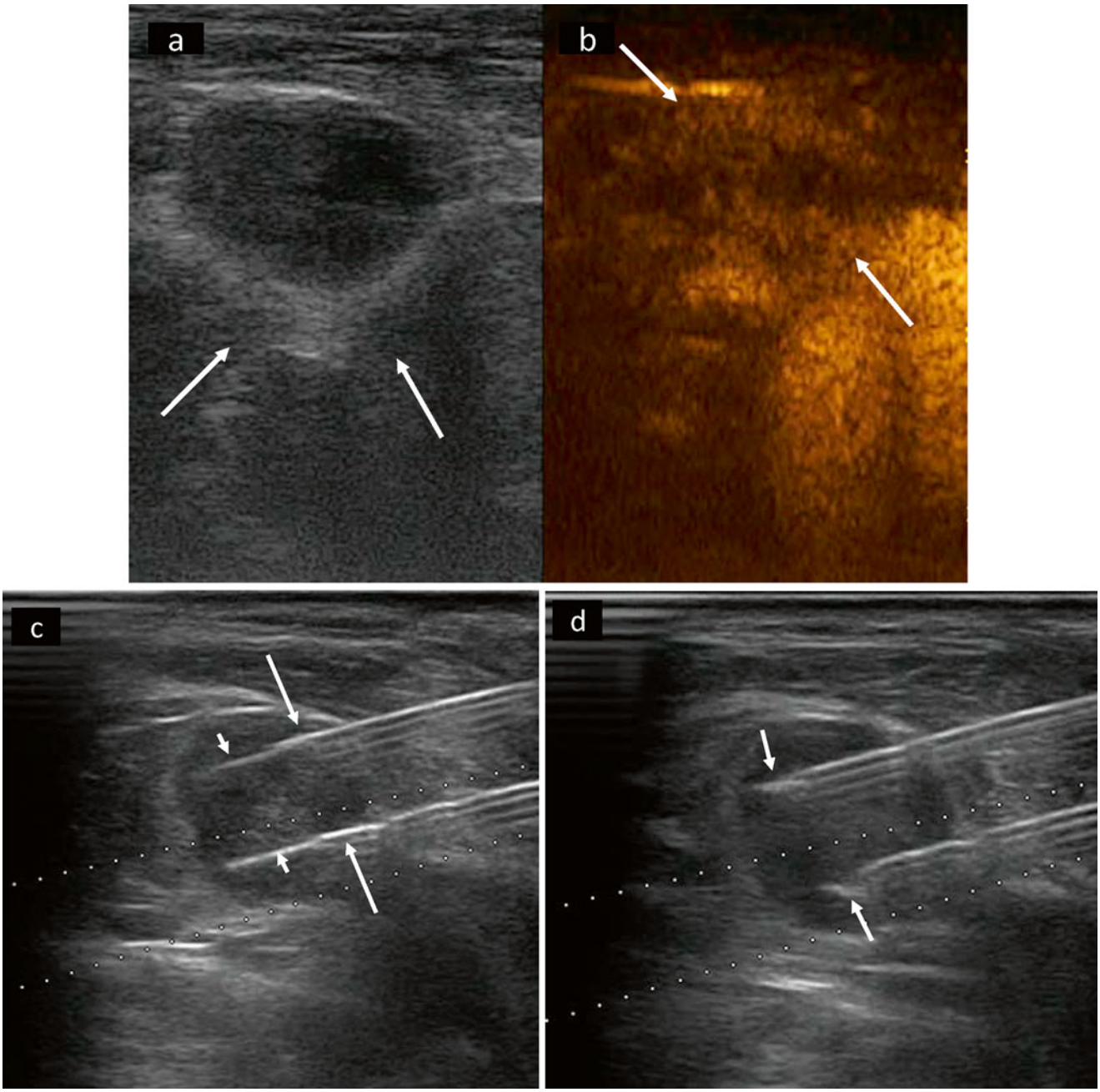

Fig. 23.10 Laser ablation (LA) for the percutaneous treatment of neck nodal metastases (NNM) from papillary thyroid cancer (PTC). (**a**) Transverse B-US image shows a metastatic neck lymph node of 2.0 cm in diameter (*arrows*), before contrast-enhanced ultrasound (CEUS). (**b**) CEUS performed before the LA procedure shows evident enhancement of the lymph node (*arrows*). (**c**) Longitudinal B-US image shows two 21G fine needles (*arrows*) and two plane-cut fibers (*arrowheads*) with interneedle spacing of 1.0 cm into the lesion at the beginning of an LA session. (**d**) Longitudinal B-US image shows the needles and the fibers during the treatment. Vapor is clearly visible (*arrow*) as small hyperechoic foci close to the tips of the fibers. (**e**) Transverse gray-scale image shows the lymph node as a hypoechoic area (*arrows*), close to the carotid artery, at the end of the LA session. (**f**) CEUS, performed after LA treatment, shows the absence of enhancement due to complete ablation of the metastatic neoplastic tissue. (**h**) 18F-FDG PET image shows marked uptake (*arrow*). (**i**) No uptake with 18F-FDG PET is visible 3 months after an LA procedure

modality, first proposed for breast lesions [107], utilizes US to evaluate the stiffness of thyroid nodules [51]. This parameter is assessed by determining the grade of distortion that occurs in a target lesion under external pressure [108]. The most common technique is to apply an external pressure on the thyroid gland using the US probe. The transducer is placed vertically over the region of interest, and a small pressure is rhythmically applied with the probe. A dedicated software compares the

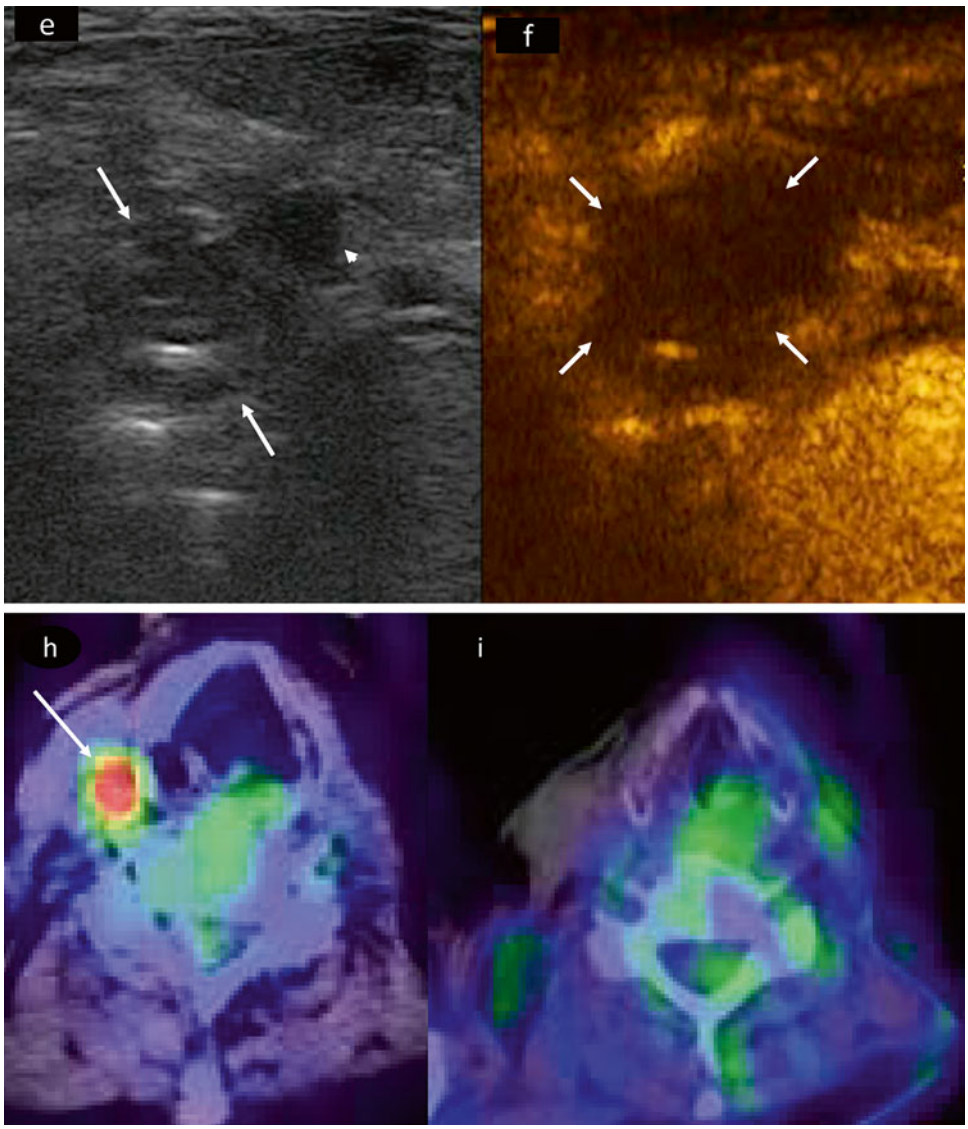

Fig. 23.10 (continued)

deformation of the lesion under evaluation to that of the surrounding parenchyma, and the relative stiffness of the lesion is illustrated by both a quantitative measure (or "strain index") and a qualitative color representation superimposed on the B-mode US image [109]. Other techniques, like the use of carotid pulsation as a compression source, are less widely used due to the frequent presence of artifacts [110].

Predictive Value of Malignancy

Thyroid Nodules

Rago et al. [111] evaluated, by real-time elastography, 96 solitary thyroid nodules that were undergoing surgery due to suspicious cytology or local pressure symptoms. Results were expressed according to a five-class qualitative score that was obtained by a subjective analysis of elastographic color images. Scores 1 and 2 were observed only in benign lesions, score 3 was observed mostly in benign nodules, and scores 4 and 5 were associated with thyroid carcinoma only. The predictive value of elastography was remarkably high. Thus, sensitivity for malignancy of scores 4–5 was 97 % with a specificity of 100 % (Fig. 23.11).

Lymph Nodes

Lyshchik et al. [112] examined 141 lymph nodes in 43 patients undergoing surgery for suspected head and neck malignancies. A strain index, calculated on the basis of lymph node versus cervical muscle stiffness, was highly predictive of malignancy. A cutoff of 1.5 was associated with a 98 % sensitivity and a 85 % specificity for malignancy. While the two [111, 112] studies demonstrated an impressively high positive predictive value of elastography in the diagnosis of malignancy, both were characterized by a num-

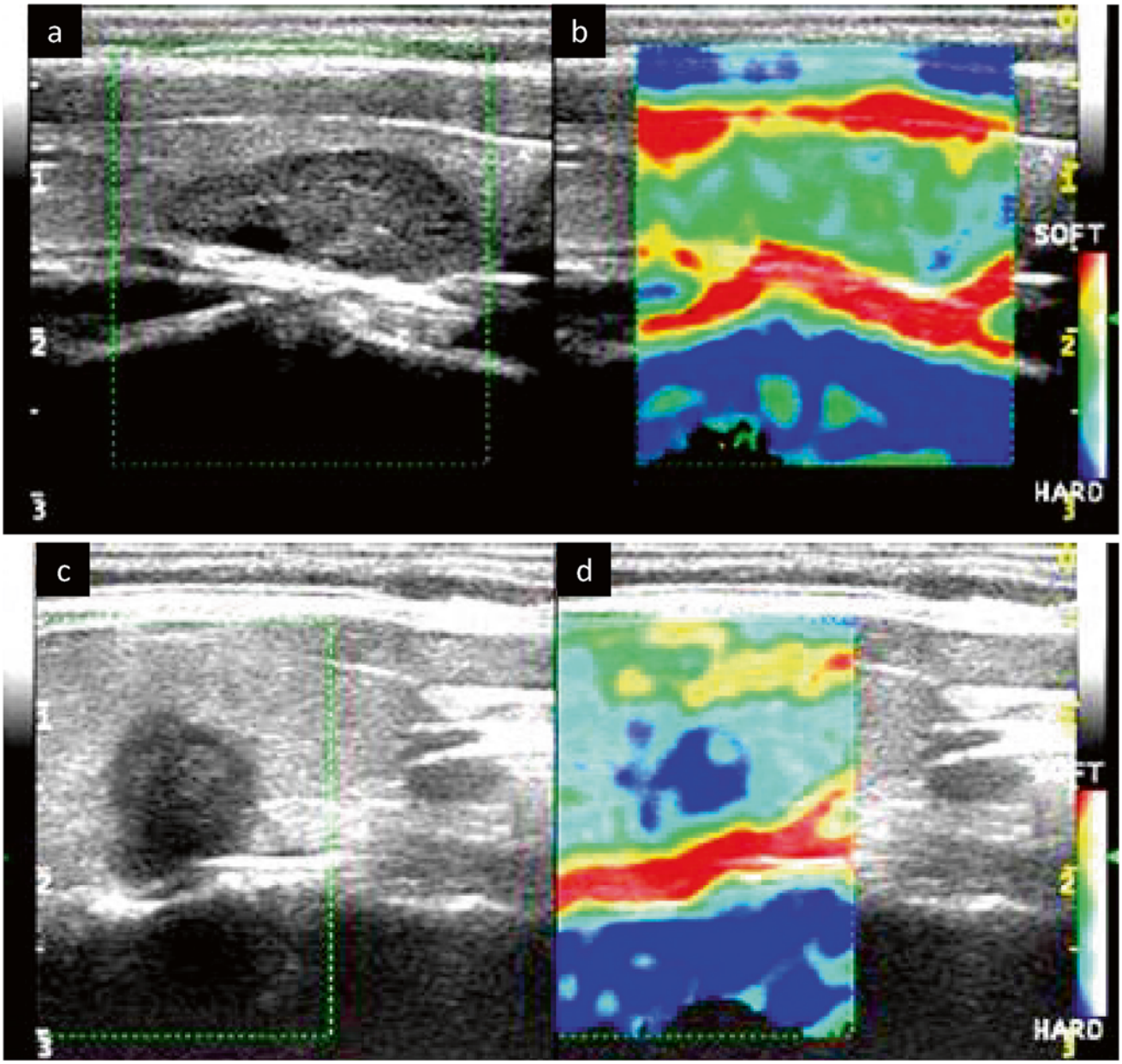

Fig. 23.11 Role of US elastography. (**a**) Sagittal conventional gray-scale image shows a thyroid nodule with US findings suggestive of a benign thyroid lesion . (**b**) US elastography image shows the nodule with elasticity score of 1. US-guided FNA confirmed the benign nature of the nodule. (**c**) Sagittal conventional B-mode US shows a marked hypoechoic nodule with irregular margins. (**d**) US elastography shows that the nodule presents an elasticity score of 5. This lesion was cytologically a papillary carcinoma

ber of shortcomings, most importantly selection bias with a very high prevalence of malignancy. Based on this, the value of elastography in a broader range of patients with nodular thyroid disease needs further evaluation [52].

Technical Limits

Elastography cannot be performed on nodules with peripheral rim calcification or intranodular macrocalcifications, due to the inability of the US beam to penetrate this hard material. Mixed nodules with a cystic component provide unreliable results because the elasticity is markedly influenced by the elasticity of the fluid component. Large size, certain localizations of the nodule(s), and abnormalities of the thyroid parenchyma (as in chronic autoimmune thyroiditis) also influence the evaluations and the value of elastography examinations [52, 109].

Clinical Use

The diagnostic accuracy of elastography for thyroid malignancy, its inter- and intraobserver reproducibility, and its cost-effectiveness, when compared with the traditional US

information, are not yet clearly established. Controlled prospective trials in larger numbers of unselected patients are needed. Hence, the use of elastography in routine clinical practice is still of limited value and remains an ancillary technique in most thyroid centers. Elastography, however, may provide rather useful information in selected clinical settings. Thus, small thyroid nodules that show nonsuspicious or indeterminate US features are usually followed up clinically without FNA. In such cases, evidence of low elasticity should strengthen the indication for FNA. A similar approach may be used for the management of cervical lymphadenopathy of uncertain significance revealed by US neck examination during follow-up of patients with thyroid carcinoma.

Contrast-Enhanced Ultrasound

Introduction

Vascularization plays a primary role in the characterization of pathologic tissue by imaging techniques. The limitations of CT and MRI in detecting density or signal differences in pathologic tissues lead to the use of iodinated contrast agents for CT and that of paramagnetic contrast agents for MRI. Similar considerations have been applied to US imaging.

The first-generation contrast medium was a simple isotonic saline solution containing air microbubbles. Second- and third-generation contrast media contain microbubbles of a gas characterized by low solubility in biologic fluids and is enclosed in lipidic or proteinous shells. These involucres increase the resistance to external pressure and provide a protracted half-life (more than 5 min for third-generation media). Contrast media are employed with US equipment and software that detect the harmonic components of the US that are scattered by microbubbles. Incident ultrasound, with a frequency close to the resonant frequency of microbubbles, starts an oscillatory motion which generates ultrasound with a dominant second harmonic component. When the receiver is tuned to this frequency, contributes from contrast media are clearly discriminated from those from solid tissues [113]. Microbubbles are small enough to pass through capillaries, and their diameter influences the resonance frequency. When a microbubble resonates, it absorbs a great quantity of the colliding energy. The microbubble becomes a scattering body which generates US waves that are spherically dispersed. If the energy is high, generated US waves are a distorted copy of the colliding ones, with a dominant frequency which is twofold that of the incident signals. The ability of microbubbles to scatter a distorted copy of the colliding energy is defined as nonlinear, or harmonic, property. Wideband transducers that can detect the harmonic response of microbubbles transmit a fundamental frequency equal to the resonance frequency of microbubbles (i.e., 2 MHz) and receive the second harmonic scattered back by the microbubbles (4 MHz). The harmonic response of contrast media is usually revealed firing sequential ultrasound impulses (typically two or three), one the inverse of the other, and then subtracting the received signals. Only the nonlinear (harmonic) component is detected. The limitations of this technique are a reduced time resolution (reduced frame rate of US scan), an increase in the transmitted energy that causes the destruction of the injected microbubbles, and the possibility of movement artifacts. The introduction of coded-pulse techniques has reduced the potential drawbacks, and currently, US equipments produce high-quality contrast-enhanced images. The usefulness of CEUS in the examination of the abdomen is established, but its use for small part examinations is still under investigation [114].

Procedure

A preliminary US evaluation of the thyroid gland should be performed, and vascular signals of the lesion should be evaluated with CD, performed with a pulse repetition frequency of 1,200, and PW, to detect slow flows. The amplifier gain should be raised until random color noise appears and then slightly lowered. The wall filter should be set low (100 Hz), and once set, the parameters should remain unchanged during the whole CEUS examination. CEUS can be performed with commercially available US scanners equipped with an electronically focused near-field linear array transducer with a 7.0–15.0 MHz bandwidth and a pulse inversion imaging software. The field of interest should be carefully selected. When possible, the area should include the carotid artery or some other major arterial vessels, the whole lesion, and a part of the surrounding normal thyroid parenchyma. The patient should be instructed not to speak or breathe deeply during the examination, and after the bolus injection, swallowing should be avoided for 2 min. After selection of the area of interest, the transducer should remain stable without modifications in its position on the neck, avoiding changes of inclination, vibrations, or involuntary movements. A precontrast clip lasting 10 s should be obtained and digitally stored in a PC-based workstation connected with or built into the US unit. A 22G peripheral intravenous needle is placed into the brachial vein, and US contrast agent is injected as a bolus in 15 s, followed by rapid flushing with 5 ml of 0.9 % saline solution. A low frame rate (5 Hz) and a very low mechanical index (MI = 0.05–0.08) should be used with the US focus placed at a lower level than the nodule under examination, in order to minimize microbubble destruction. A postcontrast clip lasting 2 min should be acquired and digitally stored for subsequent editing.

The contrast-enhancement pattern can be evaluated on the basis of:

(a) US changes at visual appearance

(b) Time-intensity curves
(c) Three-dimensional reconstruction.

Visual Appearance

Contrast enhancement may be classified as absent (no difference in enhancement between the lesion and the surrounding tissue after contrast injection), dotted (tiny scattered spots of enhancement throughout the lesion), or diffuse (homogeneous enhancement of the whole lesion). Assessment of the changes in time-intensity curves is performed at the level of regions of interest (ROI) within the nodule, the surrounding thyroid parenchyma, and the common carotid artery. Calculations of the signal intensity curves are performed using a linear scale, and results are transformed into a logarithmic scale to reduce the range of variation in the intensity values. Second-generation contrast media are devoid of human or animal substances, but a few side effects, or even rare fatal complications, have been described. The use of contrast agents is currently off label for thyroid gland visualization, and it is suggested that an informed written consent is signed by the patients. A study, performed in 2001, with a first-generation galactose-based US contrast agent claimed that the analysis of time-intensity curves was able to differentiate benign from malignant lesions [115]. A subsequent well-controlled study in 18 patients with a solitary thyroid nodule could not confirm these findings. Signal-intensity values, after the injection of a second-generation contrast medium, showed a diffuse pattern of contrast enhancement in nodules with intranodular vascular signals at baseline Doppler assessment unrelated to histological diagnoses [116]. We recently performed a blinded US study of 28 hypofunctioning solid thyroid nodules with benign, indeterminate, or malignant cytology before surgery [96]. Contrast-enhanced evaluation did not add any information to the precontrast data for the prediction of malignancy. Therefore, in our view, only future large-scale studies with surgical confirmation can clarify whether contrast-enhanced US improves the sensitivity and specificity in the selection of thyroid nodules at highest risk of harboring malignancy and whether using this technology improves the prognosis of the patients.

Clinical Use

(a) Evaluation of thyroid nodules with contrast-enhanced US (CEUS):
- Differentiation of benign from malignant lesions: visual appearance offers no advantage over conventional CD and PW.
- Time to peak, wash-in, and washout curves give no relevant information. Blood volume is reduced in small malignant lesions, but diagnostic accuracy is low and the technique is cumbersome.
- 3-D reconstruction improves visual assessment of blood volume differences and may be of aid in evaluating the risk of malignancy.

(b) Assessment of ablation treatment with CEUS seems useful for the evaluation of the extension of the coagulation zone induced by hyperthermic ablation (Fig. 23.12).

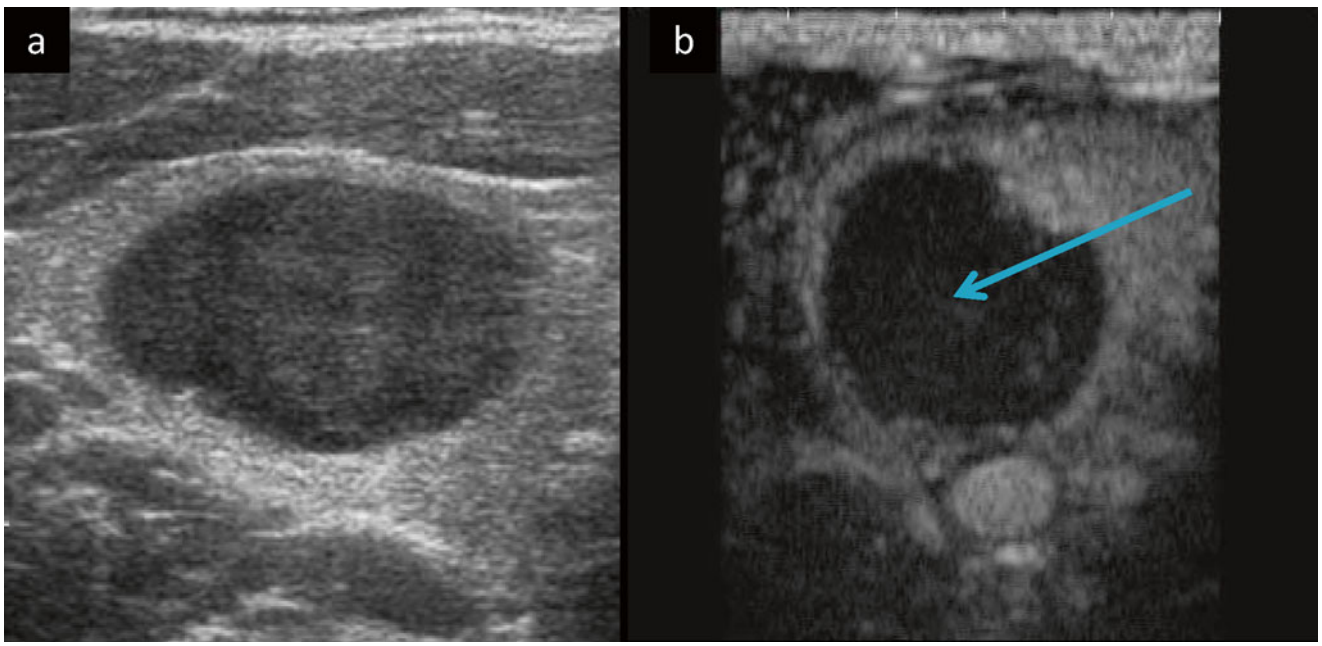

Fig. 23.12 US contrast media for the assessment of LA-induced thyroid tissue coagulation. (**a**) Transverse gray-scale image shows a solid benign nodule before LA treatment. (**b**) CEUS, 6 h after an LA session, shows a large area of coagulation (*blue arrow*) due to hyperthermic ablation

CEUS evaluation should be performed 6 h after thermal ablation to avoid the artifacts due to the presence of microbubbles of gas within the thyroid tissue. B-mode US does not provide a correct evaluation of the area of necrosis until 24 h posttherapy. Information obtained by CEUS is similar to findings by CT examination with contrast injection. However, CT is more expensive and time-consuming and requires the intravenous injection of an iodinated contrast agent.

Conclusions

First- and second-generation contrast agents seem to provide only ancillary data for the diagnosis of malignant nodules. Preliminary data using third-generation contrast media demonstrate their utility in obtaining early and valid evidence of the extent of thyroid tissue destruction induced by mini-invasive ablation procedures (laser and radiofrequency treatment) [96]. Currently, variation in time-intensity curves, during transit time of the injected microbubbles, offers only a modest improvement over prediction of malignancy provided by CD or PW evaluations [96].

References

1. Foley WD. Physical principles and instrumentation. In: Foley WD, editor. Color Doppler flow imaging. Boston: Andover Medical Publishers; 1991. p. 3–13.
2. Zagzebski J. Essentials of ultrasound physics. St Louis: Mosby; 1996.
3. Kremkau FW. Diagnostic ultrasound. Philadelphia: Saunders; 1998.
4. Goldstein A, Powis RL. Medical ultrasonic diagnostics. Phys Acoust. 1999;23:43–191.
5. Carson P. Ultrasound tissue interactions. In: Goldman L, Fowlkes J, editors. Categorical course in diagnostic radiology physics: CT and US cross-sectional imaging. Oak Brook: Radiological Society of North America; 2000. p. 9–20.
6. Bushberg J, Seibert J, Leidholdt E, Boone J. The essential physics of medical imaging. Philadelphia: Lippincott Williams & Wilkins; 2002. p. 469–553.
7. Thomenius K. Instrumentation for B-mode imaging. In: Goldman LW, Fowlles JB, editors. Categorical course in diagnostic radiology physics: CT and US cross-sectional imaging. Oak Brook: Radiological Society of North America; 2000. p. 21–32.
8. Jespersen SK, Wilhjelm JE, Sillesen H. Multi-angle compound imaging. Ultrason Imaging. 1998;20(2):81–102.
9. Burns PN. The physical principles of Doppler and spectral analysis. J Clin Ultrasound. 1987;15(9):567–90.
10. Nelson TR, Pretorius DH. The Doppler signal: where does it come from and what does it mean? AJR Am J Roentgenol. 1988;151(3):439–47.
11. Rubin JM, Bude RO, Carson PL, Bree RL, Adler RS. Power Doppler US: a potentially useful alternative to mean frequency-based color Doppler US. Radiology. 1994;190(3):853–6.
12. Stavros AT, Rapp CL, Thickman D. Sonography of inflammatory condition. Ultrasound Q. 1995;13:1–26.
13. Bude RO, Rubin JM. Power Doppler sonography. Radiology. 1996;200(1):21–3.
14. Raza S, Baum JK. Solid breast lesions: evaluation with power Doppler US. Radiology. 1997;203(1):164–8.
15. Holland SK, Orphanoudakis SC, Jaffe CC. Frequency-dependent attenuation effects in pulsed Doppler ultrasound: experimental results. IEEE Trans Biomed Eng. 1984;31(9):626–31.
16. Rizzatto G. Ultrasound transducers. Eur J Radiol. 1998;27 Suppl 2:S188–95.
17. Hegedus L, Bonnema SJ, Bennedbaek FN. Management of simple nodular goiter: current status and future perspectives. Endocr Rev. 2003;24(1):102–32.
18. Hegedus L. Clinical practice. The thyroid nodule. N Engl J Med. 2004;351(17):1764–71.
19. Hegedus L. Therapy: a new nonsurgical therapy option for benign thyroid nodules? Nat Rev Endocrinol. 2009;5(9):476–8.
20. Gharib H, Papini E, Paschke R, et al. American Association of Clinical Endocrinologists, Associazione Medici Endocrinologi, and European Thyroid Association medical guidelines for clinical practice for the diagnosis and management of thyroid nodules. J Endocrinol Invest. 2010;33(5 Suppl):1–50.
21. Gharib H, Papini E. Thyroid nodules: clinical importance, assessment, and treatment. Endocrinol Metab Clin North Am. 2007;36(3):707–35, vi.
22. American Thyroid Association Guidelines Task Force on Thyroid Nodules and Differentiated Thyroid Cancer. Haugen BR, Alexander EK, Bible KC, Doherty GM, Mandel SJ, Nikiforov YE, Pacini F, Randolph GW, Sawka AM, Schlumberger M, Schuff KG, Sherman SI, Sosa JA, Steward DL, Tuttle RM, Wartofsky L. 2015 American Thyroid Association Management Guidelines for Adult Patients with Thyroid Nodules and Differentiated Thyroid Cancer. Thyroid 2016; 26:1–133.
23. Paschke R, Hegedus L, Alexander E, Valcavi R, Papini E, Gharib H. Thyroid nodule guidelines: agreement, disagreement and need for future research. Nat Rev Endocrinol. 2011;7(6):354–61.
24. Solbiati L, Osti V, Cova L, Tonolini M. Ultrasound of thyroid, parathyroid glands and neck lymph nodes. Eur Radiol. 2001;11(12):2411–24.
25. Kwak JY, Han KH, Yoon JH, et al. Thyroid imaging reporting and data system for US features of nodules: a step in establishing better stratification of cancer risk. Radiology. 2011;260(3):892–9.
26. Moon WJ, Jung SL, Lee JH, et al. Benign and malignant thyroid nodules: US differentiation – multicenter retrospective study. Radiology. 2008;247(3):762–70.
27. Frates MC, Benson CB, Charboneau JW, et al. Management of thyroid nodules detected at US: Society of Radiologists in Ultrasound consensus conference statement. Radiology. 2005;237(3):794–800.
28. Hatabu H, Kasagi K, Yamamoto K, et al. Cystic papillary carcinoma of the thyroid gland: a new sonographic sign. Clin Radiol. 1991;43(2):121–4.
29. Watters DA, Ahuja AT, Evans RM, et al. Role of ultrasound in the management of thyroid nodules. Am J Surg. 1992;164(6):654–7.
30. Chan BK, Desser TS, McDougall IR, Weigel RJ, Jeffrey Jr RB. Common and uncommon sonographic features of papillary thyroid carcinoma. J Ultrasound Med. 2003;22(10):1083–90.
31. Hoang JK, Lee WK, Lee M, Johnson D, Farrell S. US features of thyroid malignancy: pearls and pitfalls. Radiographics. 2007;27(3):847–60; discussion 861–845.
32. Kim EK, Park CS, Chung WY, et al. New sonographic criteria for recommending fine-needle aspiration biopsy of nonpalpable solid nodules of the thyroid. AJR Am J Roentgenol. 2002;178(3):687–91.
33. Papini E, Guglielmi R, Bianchini A, et al. Risk of malignancy in nonpalpable thyroid nodules: predictive value of ultrasound and color-Doppler features. J Clin Endocrinol Metab. 2002;87(5):1941–6.
34. Yoon DY, Lee JW, Chang SK, et al. Peripheral calcification in thyroid nodules: ultrasonographic features and prediction of malignancy. J Ultrasound Med. 2007;26(10):1349–55; quiz 1356–1347.

35. Khoo ML, Asa SL, Witterick IJ, Freeman JL. Thyroid calcification and its association with thyroid carcinoma. Head Neck. 2002;24(7):651–5.
36. Peccin S, de Castsro JA, Furlanetto TW, Furtado AP, Brasil BA, Czepielewski MA. Ultrasonography: is it useful in the diagnosis of cancer in thyroid nodules? J Endocrinol Invest. 2002;25(1):39–43.
37. Kim BM, Kim MJ, Kim EK, et al. Sonographic differentiation of thyroid nodules with eggshell calcifications. J Ultrasound Med. 2008;27(10):1425–30.
38. Martinoli C, Pretolesi F, Crespi G, et al. Power Doppler sonography: clinical applications. Eur J Radiol. 1998;27 Suppl 2:S133–40.
39. Frates MC, Benson CB, Doubilet PM, Cibas ES, Marqusee E. Can color Doppler sonography aid in the prediction of malignancy of thyroid nodules? J Ultrasound Med. 2003;22(2):127–31; quiz 132–124.
40. Gharib H, Papini E, Paschke R, et al. American Association of Clinical Endocrinologists, Associazione Medici Endocrinologi, and European Thyroid Association medical guidelines for clinical practice for the diagnosis and management of thyroid nodules: executive summary of recommendations. J Endocrinol Invest. 2010;33(5 Suppl):51–6.
41. Nam-Goong IS, Kim HY, Gong G, et al. Ultrasonography-guided fine-needle aspiration of thyroid incidentaloma: correlation with pathological findings. Clin Endocrinol (Oxf). 2004;60(1):21–8.
42. Alexander EK, Marqusee E, Orcutt J, et al. Thyroid nodule shape and prediction of malignancy. Thyroid. 2004;14(11):953–8.
43. Wienke JR, Chong WK, Fielding JR, Zou KH, Mittelstaedt CA. Sonographic features of benign thyroid nodules: interobserver reliability and overlap with malignancy. J Ultrasound Med. 2003;22(10):1027–31.
44. Lee YH, Kim DW, In HS, et al. Differentiation between benign and malignant solid thyroid nodules using an US classification system. Korean J Radiol. 2011;12(5):559–67.
45. Leenhardt L, Hejblum G, Franc B, et al. Indications and limits of ultrasound-guided cytology in the management of nonpalpable thyroid nodules. J Clin Endocrinol Metab. 1999;84(1):24–8.
46. Reading CC, Charboneau JW, Hay ID, Sebo TJ. Sonography of thyroid nodules: a "classic pattern" diagnostic approach. Ultrasound Q. 2005;21(3):157–65.
47. Tamsel S, Demirpolat G, Erdogan M, et al. Power Doppler US patterns of vascularity and spectral Doppler US parameters in predicting malignancy in thyroid nodules. Clin Radiol. 2007; 62(3):245–51.
48. Moon HJ, Kwak JY, Kim MJ, Son EJ, Kim EK. Can vascularity at power Doppler US help predict thyroid malignancy? Radiology. 2010;255(1):260–9.
49. Lacout A, Marcy PY, Thariat J. RE: role of Duplex Doppler US for thyroid nodules: looking for the "sword" sign. Korean J Radiol. 2011;12(3):400–1.
50. Alexander EK, Hurwitz S, Heering JP, et al. Natural history of benign solid and cystic thyroid nodules. Ann Intern Med. 2003;138(4):315–8.
51. Lyshchik A, Higashi T, Asato R, et al. Thyroid gland tumor diagnosis at US elastography. Radiology. 2005;237(1):202–11.
52. Hegedus L. Can elastography stretch our understanding of thyroid histomorphology? J Clin Endocrinol Metab. 2010;95(12): 5213–5.
53. Duick S, Mandel S. Ultrasound-guided aspiration of thyroid nodules. In: Baskin JH, Duick DS, Levine RA, editors. Thyroid ultrasound and ultrasound-guided FNA. 2nd ed. New York: Springer Science; 2008. p. 97–110.
54. Gao J, Kazam JK, Kazam E. Imaging and biopsy guidance in the perioperative management of thyroid carcinoma. In: Carpi A, Mechanick JI, editors. Thyroid cancer: from emergent biotechnologies to clinical practice guidelines. New York: CRC Press; 2011. p. 117–32.
55. Gobien RP. Aspiration biopsy of the solitary thyroid nodule. Radiol Clin North Am. 1979;17(3):543–54.
56. Gharib H. Diagnosis of thyroid nodules by fine-needle aspiration biopsy. Curr Opin Endocrinol Diabetes. 1996;3:433–8.
57. Silverman JF, West RL, Finley JL, et al. Fine-needle aspiration versus large-needle biopsy or cutting biopsy in evaluation of thyroid nodules. Diagn Cytopathol. 1986;2(1):25–30.
58. Screaton NJ, Berman LH, Grant JW. US-guided core-needle biopsy of the thyroid gland. Radiology. 2003;226(3):827–32.
59. Zhang S, Ivanovic M, Nemecek AA, De Frias DVS, Lucas E, Nayar R. Thin core needle biopsy crush preparation in conjunction with fine-needle aspiration for the evaluation of thyroid nodules. A complementary approach. Cancer Cytopathol. 2008; 114:512–8.
60. Park KT, Ahn SH, Mo JH, et al. Role of core needle biopsy and ultrasonographic finding in management of indeterminate thyroid nodules. Head Neck. 2011;33(2):160–5.
61. Papini E, Bianchini A, Guglielmi R, et al. Image-guided minivasive ablation of thyroid tumors and distant metastases. In: Carpi A, Mechanick JI, editors. Thyroid cancer: from emergent biotechnologies to clinical practice guidelines. New York: CRC Press; 2011. p. 213–30.
62. Livraghi T, Giorgio A, Marin G, et al. Hepatocellular carcinoma and cirrhosis in 746 patients: long-term results of percutaneous ethanol injection. Radiology. 1995;197(1):101–8.
63. Solbiati L, Giangrande A, De Pra L, Bellotti E, Cantu P, Ravetto C. Percutaneous ethanol injection of parathyroid tumors under US guidance: treatment for secondary hyperparathyroidism. Radiology. 1985;155(3):607–10.
64. Charbonneau JW, Hay ID, van Heerden JA. Persistent primary hyperparathyroidism: successful ultrasound-guided percutaneous ethanol ablation of an occult adenoma. Mayo Clin Proc. 1988;63:913–7.
65. Karstrup S, Holm HH, Glenthoj A, Hegedus L. Nonsurgical treatment of primary hyperparathyroidism with sonographically guided percutaneous injection of ethanol: results in a selected series of patients. AJR Am J Roentgenol. 1990;154(5):1087–90.
66. Livraghi T, Paracchi A, Ferrari C, et al. Treatment of autonomous thyroid nodules with percutaneous ethanol injection: preliminary results. Work in progress. Radiology. 1990;175(3):827–9.
67. Bennedbaek FN, Nielsen LK, Hegedus L. Effect of percutaneous ethanol injection therapy versus suppressive doses of L-thyroxine on benign solitary solid cold thyroid nodules: a randomized trial. J Clin Endocrinol Metab. 1998;83(3):830–5.
68. Bennedbaek FN, Karstrup S, Hegedus L. Percutaneous ethanol injection therapy in the treatment of thyroid and parathyroid diseases. Eur J Endocrinol. 1997;136(3):240–50.
69. Papini E, Pacella C. Percutaneous ethanol injection of benign thyroid nodules and cysts using ultrasound. In: Baskin HJ, editor. Thyroid ultrasound and ultrasound-guided FNA biopsy. 1st ed. Boston: Kluwer Academic Publishers; 2000. p. 169–213.
70. Valcavi R, Frasoldati A. Ultrasound-guided percutaneous ethanol injection therapy in thyroid cystic nodules. Endocr Pract. 2004;10(3):269–75.
71. Guglielmi R, Pacella CM, Bianchini A, et al. Percutaneous ethanol injection treatment in benign thyroid lesions: role and efficacy. Thyroid. 2004;14(2):125–31.
72. Goletti O, Lenziardi M, De Negri F, et al. Inoperable thyroid carcinoma: palliation with percutaneous injection of ethanol. Eur J Surg. 1993;159(11–12):639–41.
73. Hay ID, Charboneau JW. The coming of age of ultrasound-guided percutaneous ethanol ablation of selected neck nodal metastases in well-differentiated thyroid carcinoma. J Clin Endocrinol Metab. 2011;96(9):2717–20.
74. Lewis BD, Hay ID, Charboneau JW, McIver B, Reading CC, Goellner JR. Percutaneous ethanol injection for treatment of cer-

vical lymph node metastases in patients with papillary thyroid carcinoma. AJR Am J Roentgenol. 2002;178(3):699–704.
75. Hay ID, Charbonneau JW, Lewis BD, et al. Successful ultrasound-guided percutaneous ethanol ablation of neck metastases in 20 patients with postoperative TNM stage I papillary thyroid carcinoma resistant to conventional therapy. (abstract). In: 74th Meeting ATA. Los Angeles; 2002. p. 176.
76. Monchik JM, Donatini G, Iannuccilli J, Dupuy DE. Radiofrequency ablation and percutaneous ethanol injection treatment for recurrent local and distant well-differentiated thyroid carcinoma. Ann Surg. 2006;244(2):296–304.
77. Lim CY, Yun JS, Lee J, Nam KH, Chung WY, Park CS. Percutaneous ethanol injection therapy for locally recurrent papillary thyroid carcinoma. Thyroid. 2007;17(4):347–50.
78. Kim BM, Kim MJ, Kim EK, Park SI, Park CS, Chung WY. Controlling recurrent papillary thyroid carcinoma in the neck by ultrasonography-guided percutaneous ethanol injection. Eur Radiol. 2008;18(4):835–42.
79. Heilo A, Sigstad E, Fagerlid KH, et al. Efficacy of ultrasound-guided percutaneous ethanol injection treatment in patients with a limited number of metastatic cervical lymph nodes from papillary thyroid carcinoma. J Clin Endocrinol Metab. 2011;96(9):2750–5.
80. Tranberg KG. Percutaneous ablation of liver tumours. Best Pract Res Clin Gastroenterol. 2004;18(1):125–45.
81. Lencioni R. Loco-regional treatment of hepatocellular carcinoma. Hepatology. 2010;52(2):762–73.
82. Dupuy DE, Monchik JM, Decrea C, Pisharodi L. Radiofrequency ablation of regional recurrence from well-differentiated thyroid malignancy. Surgery. 2001;130(6):971–7.
83. Pacella CM, Bizzarri G, Francica G, et al. Percutaneous laser ablation in the treatment of hepatocellular carcinoma with small tumors: analysis of factors affecting the achievement of tumor necrosis. J Vasc Interv Radiol. 2005;16(11):1447–57.
84. Gough-Palmer AL, Gedroyc WM. Laser ablation of hepatocellular carcinoma – a review. World J Gastroenterol. 2008;14(47):7170–4.
85. Walser EM. Percutaneous laser ablation in the treatment of hepatocellular carcinoma with a tumor size of 4 cm or smaller: analysis of factors affecting the achievement of tumor necrosis. J Vasc Interv Radiol. 2005;16(11):1427–9.
86. Pacella CM, Francica G, Di Lascio FM, et al. Long-term outcome of cirrhotic patients with early hepatocellular carcinoma treated with ultrasound-guided percutaneous laser ablation: a retrospective analysis. J Clin Oncol. 2009;27(16):2615–21.
87. Vogl TJ, Eichler K, Straub R, et al. Laser-induced thermotherapy of malignant liver tumors: general principals, equipment(s), procedure(s) – side effects, complications and results. Eur J Ultrasound. 2001;13(2):117–27.
88. Stafford RJ, Fuentes D, Elliott AA, Weinberg JS, Ahrar K. Laser-induced thermal therapy for tumor ablation. Crit Rev Biomed Eng. 2010;38(1):79–100.
89. Ahrar K, Gowda A, Javadi S, et al. Preclinical assessment of a 980-nm diode laser ablation system in a large animal tumor model. J Vasc Interv Radiol. 2010;21(4):555–61.
90. Pacella CM, Bizzarri G, Spiezia S, et al. Thyroid tissue: US-guided percutaneous laser thermal ablation. Radiology. 2004;232(1):272–80.
91. Cakir B, Topaloglu O, Gul K, et al. Ultrasound-guided percutaneous laser ablation treatment in inoperable aggressive course anaplastic thyroid carcinoma: the introduction of a novel alternative palliative therapy – second experience in the literature. J Endocrinol Invest. 2007;30(7):624–5.
92. Papini E, Guglielmi R, Hosseim G, et al. Ultrasound-guided laser ablation of incidental papillary thyroid microcarcinoma: a potential therapeutic approach in patients at surgical risk. Thyroid. 2011;21(8):917–20.
93. Solbiati L, Cova L, Ierace T, Pacella CM, Baroli A, Lomuscio G. Percutaneous US-guided interstitial laser ablation of new metastatic lymph nodes in the neck from papillary thyroid carcinoma following thyroidectomy and lymphadenectomy (abstract). In: RSNA, (ed.) 97th Scientific assembly and annual meeting. Chicago; 2011.
94. Ritz JP, Lehmann KS, Zurbuchen U, et al. Ex vivo and in vivo evaluation of laser-induced thermotherapy for nodular thyroid disease. Lasers Surg Med. 2009;41(7):479–86.
95. Pacella CM, Bizzarri G, Bianchini A, Guglielmi R, Pacella S, Papini E. US-guided laser thermal ablation of benign and malignant thyroid lesions (abstract). In: RSNA, (ed.) 84th scientific assembly and annual meeting November 30–December 5. Chicago; 2003. p. 1974.
96. Papini E, Bizzarri G, Bianchini A, et al. Contrast-enhanced ultrasound in the management of thyroid nodules. In: Baskin HJ, Duick DS, Levine RA, editors. Thyroid ultrasound and ultrasound-guided FNA. New York: Springer; 2008. p. 151–71.
97. Baek JH, Kim YS, Lee D, Huh JY, Lee JH. Benign predominantly solid thyroid nodules: prospective study of efficacy of sonographically guided radiofrequency ablation versus control condition. AJR Am J Roentgenol. 2010;194(4):1137–42.
98. Pacella CM, Bizzarri G, Guglielmi R, et al. Thyroid tissue: US-guided percutaneous interstitial laser ablation-a feasibility study. Radiology. 2000;217(3):673–7.
99. Dossing H, Bennedbaek FN, Hegedus L. Ultrasound-guided interstitial laser photocoagulation of an autonomous thyroid nodule: the introduction of a novel alternative. Thyroid. 2003;13(9):885–8.
100. Dossing H, Bennedbaek FN, Hegedus L. Effect of ultrasound-guided interstitial laser photocoagulation on benign solitary solid cold thyroid nodules – a randomised study. Eur J Endocrinol. 2005;152(3):341–5.
101. Papini E, Guglielmi R, Bizzarri G, et al. Treatment of benign cold thyroid nodules: a randomized clinical trial of percutaneous laser ablation versus levothyroxine therapy or follow-up. Thyroid. 2007;17(3):229–35.
102. Dossing H, Bennedbaek FN, Hegedus L. Long-term outcome following interstitial laser photocoagulation of benign cold thyroid nodules. Eur J Endocrinol. 2011;165(1):123–8.
103. Esnault O, Franc B, Menegaux F, et al. High-intensity focused ultrasound ablation of thyroid nodules: first human feasibility study. Thyroid. 2011;21(9):965–73.
104. Kovatcheva RD, Vlahov JD, Shinkov AD, et al. High-intensity focused ultrasound to treat primary hyperparathyroidism: a feasibility study in four patients. AJR Am J Roentgenol. 2010;195(4):830–5.
105. Lerner RM, Huang SR, Parker KJ. "Sonoelasticity" images derived from ultrasound signals in mechanically vibrated tissues. Ultrasound Med Biol. 1990;16(3):231–9.
106. Konofagou EE. Quo vadis elasticity imaging? Ultrasonics. 2004;42(1–9):331–6.
107. Itoh A, Ueno E, Tohno E, et al. Breast disease: clinical application of US elastography for diagnosis. Radiology. 2006;239(2):341–50.
108. Lyshchik A, Higashi T, Asato R, et al. Elastic moduli of thyroid tissues under compression. Ultrason Imaging. 2005;27(2):101–10.
109. Levine RA. Ultrasound elastography of the thyroid. In: Baskin J, Duick D, Levine R, editors. Thyroid ultrasound and ultrasound-guided FNA. 2nd ed. New York: Springer Science; 2008. p. 237–43.
110. Bae U, Dighe M, Dubinsky T, Minoshima S, Shamdasani V, Kim Y. Ultrasound thyroid elastography using carotid artery pulsation: preliminary study. J Ultrasound Med. 2007;26(6):797–805.
111. Rago T, Santini F, Scutari M, Pinchera A, Vitti P. Elastography: new developments in ultrasound for predicting malignancy in thyroid nodules. J Clin Endocrinol Metab. 2007;92(8):2917–22.

112. Lyshchik A, Higashi T, Asato R, et al. Cervical lymph node metastases: diagnosis at sonoelastography – initial experience. Radiology. 2007;243(1):258–67.
113. Wilson SR, Burns PN. Microbubble contrast for radiological imaging: 2. Applications. Ultrasound Q. 2006;22(1):15–8.
114. Huang-Wei C, Bleuzen A, Bourlier P, et al. Differential diagnosis of focal nodular hyperplasia with quantitative parametric analysis in contrast-enhanced sonography. Invest Radiol. 2006;41(3):363–8.
115. Spiezia S, Farina R, Cerbone G, et al. Analysis of color Doppler signal intensity variation after levovist injection: a new approach to the diagnosis of thyroid nodules. J Ultrasound Med. 2001;20(3):223–31; quiz 233.
116. Bartolotta TV, Midiri M, Galia M, et al. Qualitative and quantitative evaluation of solitary thyroid nodules with contrast-enhanced ultrasound: initial results. Eur Radiol. 2006;16(10):2234–41.